Published for SISSA by Springer

Received: December 18, 2019
Revised: August 7, 2020
Accepted: August 15, 2020
Published: September 29, 2020

Supersymmetric phases of 4d $\mathcal{N} = 4$ SYM at large N

Alejandro Cabo-Bizet and Sameer Murthy

Department of Mathematics, King's College London,
The Strand, London WC2R 2LS, U.K.

E-mail: alejandro.cabo_bizet@kcl.ac.uk, sameer.murthy@kcl.ac.uk

Abstract: We find a family of complex saddle-points at large N of the matrix model for the superconformal index of SU(N) $\mathcal{N} = 4$ super Yang-Mills theory on $S^3 \times S^1$ with one chemical potential τ. The saddle-point configurations are labelled by points (m, n) on the lattice $\Lambda_\tau = \mathbb{Z}\tau + \mathbb{Z}$ with $\gcd(m, n) = 1$. The eigenvalues at a given saddle are uniformly distributed along a string winding (m, n) times along the (A, B) cycles of the torus $\mathbb{C}/\Lambda_\tau$. The action of the matrix model extended to the torus is closely related to the Bloch-Wigner elliptic dilogarithm, and the related Bloch formula allows us to calculate the action at the saddle-points in terms of real-analytic Eisenstein series. The actions of $(0, 1)$ and $(1, 0)$ agree with that of pure AdS_5 and the supersymmetric AdS_5 black hole, respectively. The black hole saddle dominates the canonical ensemble when τ is close to the origin, and there are new saddles that dominate when τ approaches rational points. The extension of the action in terms of modular forms leads to a simple treatment of the Cardy-like limit $\tau \to 0$.

Keywords: AdS-CFT Correspondence, Black Holes in String Theory, Supersymmetric Gauge Theory

ArXiv ePrint: 1909.09597

https://doi.org/10.1007/JHEP09(2020)184

JHEP09(2020)184

Contents

1 Introduction

The subject of this paper is a matrix model defined by an integral over $N \times N$ unitary matrices U of the following type,

$$\mathcal{I}(\vec{\tau}) = \int DU \, \exp\left(\sum_{n=1}^{\infty} \frac{1}{n} f(n\vec{\tau}) \operatorname{tr} U^n \operatorname{tr} (U^\dagger)^n \right). \tag{1.1}$$

JHEP09(2020)184

Here $\vec{\tau}$ denotes the vector of coupling constants of the model, and DU is the invariant measure. Upon diagonalizing the matrices, one obtains an integral over the N eigenvalues which experience a purely two-particle interaction governed by the single function $f(\vec{\tau})$. The particular model that we analyze arises as the generating function of the superconformal index [1, 2] of $\mathcal{N} = 4$ super Yang-Mills (SYM) theory on $S^3 \times S^1$. In this model U has the interpretation as the holonomy of the gauge field around S^1, and there are three coupling constants τ, σ, φ, which are interpreted, respectively, as the chemical potentials dual to the two angular momenta on the S^3 and a certain combination of the R-charges of the theory. The function f has the interpretation as the single-letter index of the super Yang-Mills theory [1].

The matrix model (1.1) for the supersymmetric index has generated a lot of interest since the work of [2]. The holographically dual gravitational theory with AdS_5 boundary conditions admits supersymmetric black hole solutions which preserve the same supercharges as the superconformal index $\mathcal{I}$ captured by the matrix model. This leads to the expectation that the (indexed) degeneracies of states contained in $\mathcal{I}$ grow exponentially as a function of the charges when the charges become large enough to form a black hole. The analysis of [2] seemed to suggest that the shape, or functional form, of $\mathcal{I}$ does not allow for such a growth of states, thus leading to a long-standing puzzle.

Following the insightful observation of [3], this puzzle has been revisited recently [4–21] The emergent picture shows that there is actually an exponential growth of states contained in the index, which is captured by the saddle-point estimate if one allows the potentials σ, τ, φ to take values in the complex plane away from the pure imaginary values assumed in [2].[1] There are essentially three strands of analysis contained in the recent progress:

1. The first strand is an analysis of the bulk supergravity [4] which shows that the black hole entropy can be understood as the Legendre transform of the regularized on-shell action of a family of Euclidean solutions lying on the surface

$$\sigma + \tau - 2\varphi = n_0 \,, \qquad n_0 = -1 \,. \tag{1.2}$$

   It was first noticed in [3] that this constraint is important to obtain the black hole entropy as an extremization of an entropy function. The result of [4] gives a physical interpretation to this observation — the entropy function is the gravitational action, and the constraint arises from demanding supersymmetry. One is thus led to look at configurations on this surface in the field theory index in order to make accurate saddle-points estimates.

2. The second strand, referred to as the Cardy-like limit [5, 10, 11, 13, 14] is the analysis of the index $\mathcal{I}$ in the limit when the charges are much larger than all other parameters of the theory including N. In the bulk gravitational dual, this corresponds to a black hole that "fills up all of AdS space". In this limit one finds a configuration of eigenvalues clumped near the origin which has an entropy equal to that of the black

[1] If we restrict all three potentials to be purely imaginary, these analyses also show that there is no growth of states at large N, as consistent with the analysis of [2].

JHEP09(2020)184

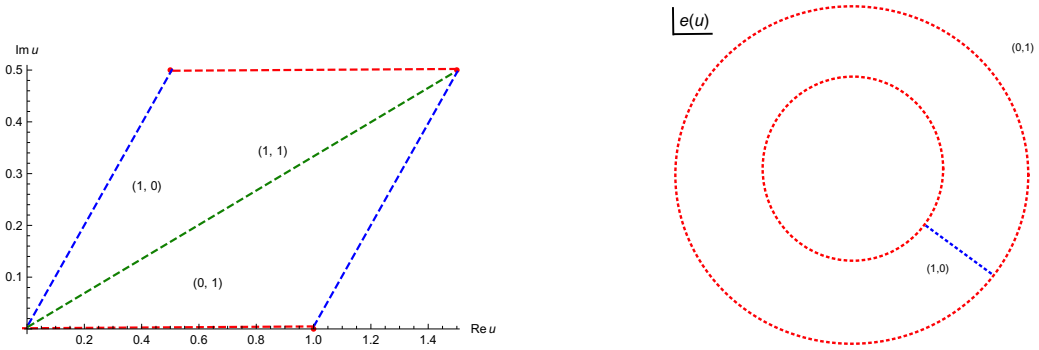

Figure 1. The saddle-point configurations of eigenvalues in the fundamental domain and on the torus for $\tau = \frac{1}{2}(1+\mathrm{i})$. The saddles shown are $(0,1)$ (red), $(1,0)$ (blue), and $(1,1)$ (green). The original definition of the matrix model is the interval $[0,1)$ on the left which maps to the outer circle of unit radius on the right.

hole. This analysis has some subtleties related to convergence of infinite sums and the related puzzle that if one literally puts all the eigenvalues at the origin then the index seems to vanish. The resolution is given by a certain limiting procedure in which the eigenvalues are placed close to zero and one then takes the limit of the entropy as they go to zero.

3. The third strand is the Bethe-ansatz analysis for the subspace $\tau = \sigma$, initiated by [7, 8]. Here the analysis is performed not directly on the matrix model (1.1) but on an equivalent representation of the index [7, 22, 23] which one can solve at large N by computing the roots of the Bethe-ansatz equations. These roots are referred to in [8] as saddle-point-like configurations, suggesting that those configurations could correspond to the saddle-points of the matrix model (1.1). This analysis was shown in [8] to be consistent with that of Point 2 when one further takes the Cardy-like limit.

Put together, these three strands of analysis strongly suggest that there should be a complex saddle-point of the matrix model (1.1) at large N and finite τ, having the same entropy as that of the black hole. In this paper we show that this is indeed the case in the subspace of coupling constants $\sigma = \tau$. Within this subspace we find an infinite family of saddle-points labelled by points on the lattice $\Lambda_\tau = \mathbb{Z}\tau + \mathbb{Z}$. More precisely, writing a generic lattice point as $m\tau + n$, $m, n \in \mathbb{Z}$, the independent saddles are labelled by (m, n) with $\gcd(m, n) = 1$. As we explain below, our solution is best presented in terms of the torus $\mathbb{C}/\Lambda_\tau$ whose A-cycle is identified with the original circle of unit radius. The eigenvalues at the (m, n) saddle are uniformly distributed along a string winding m and n times along the A and B cycles, respectively, of the torus (see figure 1). In particular, the saddle $(0, 1)$ is identified with pure AdS_5 and $(1, 0)$ is identified with the supersymmetric AdS_5 black hole.

Our method of analysis is as follows. Firstly we need to extend the action to complex values of the fields. Denoting the eigenvalues of the matrix U as $e^{2\pi \mathrm{i} u_i}$, $i = 1, \ldots, N$, the variables u_i of the original unitary matrix model take values in $\mathbb{R}/\mathbb{Z}$, whose representative

JHEP09(2020)184

we choose throughout the paper to be $[0, 1)$. "Complex field configurations" in our context means complex values of u_i or, equivalently, moving away from the original circle of unit radius in the variables $e^{2\pi i u_i}$. A priori there is no canonical manner to extend the action to the complex plane. A natural first guess may be to use the analytic continuation of the original action away from real values of u_i. However, the construction of our solution needs the action to be well-defined on the torus, for which the analytic continuation is not the right choice as it is only quasi-periodic under translations $u_i \to u_i + \tau$ (in a manner that generalizes the quasi-periodicity of the Jacobi θ-function). The good choice of continuation of the action to the complex u_i plane turns out to be a doubly periodic function, i.e. one which is strictly periodic under translations of 1 and τ. This function is not meromorphic but (with a small abuse of terminology) we shall sometimes call it an elliptic function. This choice can be thought of as a real-analytic (in u) deformation of the analytic continuation which cures the "small" non-periodicity at the expense of meromorphy.

The fact that the extended action is not meromorphic gives rise to new subtleties compared to the saddle-point analysis for meromophic functions. Firstly we need to find solutions to the variational equations in the real and imaginary directions separately. It is actually quite easy to see that any periodic uniform distribution of eigenvalues in the complex plane solves the saddle-point equations, and we present this as a Lemma in section 2. Secondly, we need a separate argument to justify the contour deformation so that it passes through the saddle-points. In section 3.3 we show that we can replace the doubly-periodic integrand by a meromorphic integrand without changing the large-N value of the corresponding integrals on the original contour as well as on a contour passing through the saddle-point. We can thus use the meromorphicity to deform the contour, modulo issues of wall-crossings that we do not analyze here. Thirdly, we need to consider the space of all contours and analyze the contribution of a given saddle-point as a function of the moduli of the theory. We do not address this last issue in this paper. We note, however, that, since the contour deformation argument relies on an associated meromorphic function, it may be possible to adapt the formalism of Picard-Lefschetz theory and the ideas of resurgence to our case (a recent comprehensive review of this subject can be found in [28]).

The particular elliptic function that underlies our extended action can be identified with the *elliptic dilogarithm*, a certain single-valued real-analytic extension of the ordinary dilogarithm first studied by D. Wigner and S. Bloch [24]. This identification immediately places us in a very good position. The main technical tool is a formula due to Bloch [24] which has been studied intensively by number theorists [25, 26]. Bloch's formula expresses the elliptic dilogarithm in terms of a real analytic lattice sum also known as a Kronecker-Eisenstein series [27], which is not only manifestly elliptic but also modular invariant under the usual $SL_2(\mathbb{Z})$ action on τ! The Kronecker-Eisenstein series can be thought of as a Fourier expansion along the lattice directions, and this makes the calculation of the action at the saddle-points very easy as we just have to calculate the zeroth Fourier modes along the direction chosen by a given lattice point.

In section 4 we calculate the resulting actions of the $(0, 1)$ and $(1, 0)$ saddles, and find that they agree precisely with that of pure AdS_5 and the supersymmetric AdS_5 black hole, respectively. This leads us to the above-mentioned identification of these saddles as the

JHEP09(2020)184

duals of the respective gravitational configurations. We also calculate the action and the entropy of the generic (m, n) saddle. Comparing the various actions at a given value of τ, we calculate the resulting phase diagram for the supersymmetric theory. (The bounding curves of the resulting regions are the anti-Stokes lines.) We find that the dominant phase close to $\tau = 0$ is the AdS_5 black hole. In addition, when τ approaches the rational point $-n/m$, the (m, n) solution becomes dominant. These are new supersymmetric phases of the theory.

The form of the Kronecker-Eisenstein series allows us to easily calculate the asymptotics of the action at a given saddle-point in the Cardy-like limit $\tau \to 0$. Applying this procedure to the black hole saddle immediately yields the leading terms in the limit, thus clarifying certain technical issues that arose in the calculations in the Cardy-like limit in [14] by different methods.[2] Our formalism thus unifies the three strands of analysis mentioned above and confirms the following satisfying physical picture of the Cardy-like limit — it is simply the limit when the black hole saddle-point shrinks to zero size, i.e. the configuration of eigenvalues uniformly distributed between 0 and τ all coalesce to the origin.

Finally, we make contact with the results of the Bethe-ansatz approach. In that approach, one directly considers the integral of a product of elliptic gamma-functions which is a meromorphic function of u_i. The uniform distribution of eigenvalues in the (m, n) configuration are known to be roots of the Bethe-ansatz equations [8]. The effective action of the meromorphic integrand was calculated in [8] on the $(1, n)$ configurations, but had not been calculated previously for $m > 1$. In order to compare our results for the bigger family, we develop a new method to calculate the meromorphic effective action at a generic (m, n) configuration, by rewriting the elliptic gamma function as an infinite series, convergent along the direction of a given lattice point. For all (m, n) configurations, we find that the results of the elliptic approach and the Bethe-ansatz approach agree. In order to illustrate this agreement in a slightly different way, we also calculate the difference between the two effective actions and directly show that this (non-periodic) difference vanishes on any (m, n) configuration (see section 3.3 and appendices C and E).

The plan of the paper is as follows. In section 2 we present a simple lemma which allows us to find complex saddle-point configurations for a class of matrix models defined purely by a two-particle potential. We also briefly review the index for $\mathcal{N} = 4$ SYM on $S^1 \times S^3$ and its integral representation in terms of elliptic gamma functions Γ_e. In section 3 we show how to extend the action of the matrix model from the unit circle to a torus using the elliptic dilogarithm. In section 4 we calculate the action and the entropy of a generic saddle and discuss the phase structure of our supersymmetric matrix model. We also make some comments about the Cardy-like limit. In section 5 we make some brief comments about interesting aspects of this problem that we do not discuss in this paper. In appendices A–F we collect the definitions and useful properties of the various functions that enter in our analysis, discuss the analytic continuation of the integrand of the index and its relation with our elliptic extension, and use this discussion to recover our previous results and compare them with the Bethe-ansatz approach.

[2] Preliminary indications of modular invariance in related systems were found in [29–33]. The calculations of [4], which showed that a generalized supersymmetric Casimir energy of $\mathcal{N} = 4$ SYM on $S^1 \times S^3$ equals the black hole entropy functional, also pointed towards a modular symmetry underlying the system.

JHEP09(2020)184

Notation. We will use the notation $\mathbf{e}(x) \coloneqq \mathrm{e}^{2\pi \mathrm{i} x}$ throughout the paper: we will use $\tau \in \mathbb{H}$ as the modular parameter and $z, u \in \mathbb{C}$ as elliptic variables. We set $q = \mathbf{e}(\tau)$, $\zeta = \mathbf{e}(z)$. We decompose the modular variable into its real and imaginary parts as $\tau = \tau_1 + \mathrm{i}\tau_2$, and the elliptic variables into their projections on to the basis $(1, \tau)$, i.e. $z_2 = \frac{\mathrm{Im}(z)}{\tau_2}$, $z_1 = \mathrm{Re}(z) - z_2\,\tau_1$ so that $z = z_1 + \tau z_2$. $\mathbb{N}$ denotes the set of natural numbers and $\mathbb{N}_0 = \mathbb{N} \cup \{0\}$.

2 Complex saddle-points of $\mathcal{N} = 4$ SYM

In this section we present a simple lemma which allows us to find complex saddle-point configurations for matrix integrals of the type (1.1). Upon rewriting these integrals in terms of eigenvalues, the class of models that we consider have no single-particle interactions, and only two-particle interactions which depend only on the distance between the two particles. With these assumptions the basic lemma states that if the potential is periodic in any (complex) direction in field space then the uniform distribution between the origin and the point of periodicity is a saddle-point. We then review some properties of the $\mathcal{N} = 4$ superconformal index and set up the particular problem of interest to us.

2.1 Saddle-point configurations for periodic potentials

As is well-known, the matrix integral Z in (1.1) reduces to an integral over the eigenvalues of U which we denote by $\{\mathbf{e}(u_i)\}_{i=1,\ldots,N}$. The product of two traces in (1.1) leads to an overall N^2 in front of the action, which allows us to use large-N methods. In the large-N limit one promotes $\{u_i\}$ to a continuous variable $u(x)$, $x \in [0,1]$, and replaces the sum over i by an integral over x. One can further replace each integral over x in the action by an integral over u with a factor of the eigenvalue density $\rho(u) = \frac{dx}{du}$ which obeys the normalization condition $\int du\, \rho(u) = 1$. In this limit the integral (1.1) can be written in terms of an effective action $S(u)$ as

$$Z = \int [Du]\, \exp\bigl(-S(u)\bigr)\,, \qquad S = N^2 \int du\, dv\, \rho(u)\, \rho(v)\, V(u-v)\,, \tag{2.1}$$

where the pairwise potential V is determined by the function $f(\tau)$. The paths $u(x)$ run over the real interval $(-\frac{1}{2}, \frac{1}{2}]$ in the unitary matrix model, but here we are interested in complex saddle-points of this model. The main observation is that if the pairwise potential $V(z)$ is periodic with (complex) period T, then the uniform distribution $u(x) = xT$, $x \in [0,1]$, extremizes the effective action. To see this we first note that the odd part of the potential $\frac{1}{2}(V(u) - V(-u))$ drops out of the integral in (2.1)), and so $V(u)$ can be taken to be an even function. Now, the variational equations arising from the integral (2.1) are

$$\int dv\, \partial_z V(u-v)\, \rho(v) = 0\,, \qquad \int dv\, \partial_{\bar{z}} V(u-v)\, \rho(v) = 0\,. \tag{2.2}$$

The partial derivatives here are odd, periodic functions with period T. On the configuration $u(x) = xT$, the left-hand side of this equation equals $\frac{1}{T}\int_0^T dv\, V'(u-v)$ where the integral is understood to be along a straight line in the complex plane along 0 to T. Using

JHEP09(2020)184

the periodicity and oddness properties, respectively, we now have (with $'$ denoting either the holomorphic or anti-holomorphic derivative),

$$\frac{1}{T}\int_0^T dv\, V'(u-v) = -\frac{1}{T}\int_{-T/2}^{T/2} dw\, V'(w) = 0\,. \tag{2.3}$$

This same argument, with minor changes, can be repeated in the discrete variables. We present this as a lemma which we will use in the following development. Here we set $\underline{u} \equiv \{u_i\}_{i=1,\ldots,N}$, and use the measure $[D\underline{u}] = \frac{1}{N!}\prod_{i=1}^N \mathrm{d}u_i$. We will work with the SU(N) gauge theory throughout the paper for which we need to include the tracelessness condition $\sum_{i=1}^N u_i = 0$. Consider the N-dimensional integral defined by a pairwise potential between the eigenvalues that only depends on the difference $u_{ij} = u_i - u_j$, i.e.,

$$Z = \int [D\underline{u}]\exp\bigl(-S(\underline{u})\bigr)\,, \qquad S(\underline{u}) = \sum_{i,j=1}^N V(u_{ij})\,. \tag{2.4}$$

We take the potential $V(z)$ to be any smooth complex-valued function, not necessarily meromorphic. A question about contour-deformations immediately arises.[3] When the integrand is holomorphic we can freely change the contour so as to pass through complex saddle-points. Since we are not demanding holomorphicity, we need an additional argument to be able to deform the contour to pass through the saddle-point. We are able to do this in the context of the specific functions discussed later in this paper, as we elaborate in section 3.3. Now we consider the variational equations

$$\partial_{u_i} S(\underline{u}) = \partial_{\overline{u}_i} S(\underline{u}) = 0\,, \qquad i = 1,\ldots,N\,. \tag{2.5}$$

Lemma. In the above set up, suppose the potential V is periodic with (complex) period T. Then

(i) The following configuration solves the variational equations (2.5),

$$u_i = \frac{i}{N}\,T + u_0\,, \tag{2.6}$$

where u_0 is fixed in such a way the traceless constraint is obeyed.

(ii) The action $S(\underline{u})$ at the saddle (2.6) is given by N^2 times the average value of the potential on the straight line joining 0 and T in the large-N limit.

Remark. The distribution (2.6) becomes the uniform distribution between 0 and T in the large-N limit. Since the potential V is periodic with period T, it admits a Fourier expansion along that direction. The second part of the lemma is equivalent to saying that the saddle-point value of the action is N^2 times the zeroth Fourier coefficient in the direction T.

[3] We thank the referee for emphasizing this point.

JHEP09(2020)184

To prove the first part of the lemma, we assume, without loss of generality as before, that V is an even function. The saddle-point equations (2.5) can be written as

$$\sum_{j\neq i} \partial_z V(u_{ij}) = 0\,, \qquad \sum_{j\neq i} \partial_{\bar z} V(u_{ij}) = 0\,. \tag{2.7}$$

On the configuration (2.6) we have $u_{ij} = (i-j)T/N$. For every point j in this sum the point $j' = 2i - j\,(\mathrm{mod}N)$ is equidistant from i and lives on the other side of i, that is $i - j = -(i-j')\,(\mathrm{mod}N)$. Since the functions $\partial_z V$, $\partial_{\bar z} V$ are odd and periodic with period T, these two points cancel against each other and the sums in (2.7) vanish. (For even N the antipodal point $i + \frac{1}{2}N\,(\mathrm{mod}N)$ is its own partner, but the argument still applies as $\partial_z V(T/2) = \partial_{\bar z} V(T/2) = 0$.)

The second part of the lemma follows from a simple calculation of the action on the distribution (2.6), which we call the *effective action* of the saddle:

$$S_{\text{eff}}(T) = \sum_{i,j=1}^{N} V\Big(\frac{i-j}{N}T\Big) = \sum_{i,j=1}^{N} V\Big(\frac{i}{N}T\Big) = N\sum_{i=1}^{N} V\Big(\frac{i}{N}T\Big) = N^2\int_0^1 dx\, V(xT)\,. \tag{2.8}$$

In obtaining the second equality we have used the periodicity of the potential, and in the last equality we have used the large-N limit. □

2.2 The index of $\mathcal{N} = 4$ SYM

The superconformal index of $\mathcal{N} = 4$ SYM theory was calculated in [1, 2]. In [4] this index was revisited as a path integral corresponding to the partition function of supersymmetric field theories on $S^3 \times S^1$ with complexified angular chemical potentials σ, τ for rotation in S^3, and holonomy for the background R-symmetry gauge field A given by $\int_{S^1} A = \mathrm{i}\pi\varphi$, with $\varphi = \mathrm{i}(\sigma + \tau - n_0)$. The introduction of the integer n_0 in [4] corresponds to a shift in the background value of the R-symmetry gauge field.[4] It was shown in [4] that

$$\mathcal{I}(\sigma,\tau;n_0) = \mathcal{I}(\sigma - n_0,\tau;0)\,, \tag{2.9}$$

where the function $\mathcal{I}(\sigma,\tau;0)$ is the familiar Hamiltonian definition of the superconformal index [1, 2]

$$\mathcal{I}(\sigma,\tau;0) = \mathrm{Tr}_{\mathcal{H}_{\text{phys}}}\,(-1)^F \mathrm{e}^{-\beta\{\mathcal{Q},\bar{\mathcal{Q}}\}+2\pi\mathrm{i}\sigma(J_1+\frac{1}{2}Q)+2\pi\mathrm{i}\tau(J_2+\frac{1}{2}Q)}\,. \tag{2.10}$$

The above two equations make two things immediately clear. On one hand they show that the index $\mathcal{I}(\tau,\sigma;n_0)$ is protected against small deformations of the parameters of the theory exactly as the original index. On the other hand expanding the index as

$$\mathcal{I}(\sigma,\tau;n_0) = \sum_{n_1,n_2} d(n_1,n_2;n_0)\,\mathrm{e}^{2\pi\mathrm{i}(\sigma n_1+\tau n_2)} \tag{2.11}$$

in terms of the degeneracies $d(n_1,n_2)$, we see from (2.10) that a constant shift of the chemical potentials only changes the phase of the indexed degeneracies, so that

$$|d(n_1,n_2;n_0)| = |d(n_1,n_2;0)|\,. \tag{2.12}$$

[4] Equivalently the fermions can be thought of as antiperiodic with the unshifted gauge field values.

JHEP09(2020)184

Thus we have that the index $\mathcal{I}$, i.e. the canonical partition function, depends on n_0 whose correct value is dictated by the holographic dictionary. For the degeneracies d, i.e. the microcanonical observables, the value of n_0 does not change the absolute value of the degeneracies. It does, however, play a role in the calculation of the saddle-point value of the degeneracies as a function of large charges, since a change of n_0 corresponds to a change in the τ-contour of integration used to define the saddle-point value, and for the purpose of this calculation one should use a value of n_0 that maximizes the answer. In our situation, since the R-charges of the $\mathcal{N}=4$ SYM theory are quantized in units of $\frac{1}{3}$, the degeneracies only depend on n_0 (mod 3). We can choose the representatives to be $n_0 = 0, \pm 1$. As it turns out, the natural contours associated to $n_0 = \pm 1$ both have leading entropy at large charges equal to that of the black hole, which dominates the natural contour associated to $n_0 = 0$. We note that one can map $n_0 = +1 \mapsto n_0 = -1$ by using the transformation $(\mathrm{Re}\,\sigma, \mathrm{Re}\,\tau) \to -(\mathrm{Re}\,\sigma, \mathrm{Re}\,\tau)$. All this is consistent with the supergravity calculation of the Euclidean black hole [4]. We will use the value $n_0 = -1$ in the rest of the paper and suppress writing it explicitly.

The superconformal index of SU(N) $\mathcal{N}=4$ SYM can be written in the form (1.1) with

$$f(\sigma,\tau) = 1 - \frac{\left(1-\mathbf{e}\left(\frac{1}{3}(\sigma+\tau+1)\right)\right)^3}{\left(1-\mathbf{e}(\tau)\right)\left(1-\mathbf{e}(\sigma)\right)}\,. \tag{2.13}$$

One can recast the exponential of the infinite sum expression in (1.1) in terms of an infinite product to obtain the following N-dimensional integral, [4, 34]

$$\begin{aligned}\mathcal{I}(\sigma,\tau) = \left(\mathbf{e}(-\tfrac{\sigma}{24}-\tfrac{\tau}{24})\,\eta(\sigma)\,\eta(\tau)\right)^N \times \\ \int [D\underline{u}] \prod_{i\neq j} \Gamma_{\mathrm{e}}\left(u_{ij}+\sigma+\tau;\sigma,\tau\right) \prod_{i,j} \Gamma_{\mathrm{e}}\left(u_{ij}+\frac{1}{3}(\sigma+\tau-n_0);\sigma,\tau\right)^3\,,\end{aligned} \tag{2.14}$$

where the measure factor is $[D\underline{u}] = \frac{1}{N!}\prod_{i=1}^N \mathrm{d}u_i\,\delta\left(\sum_i u_i\right)$ and the integral over each u_i runs over the real range $(-\frac{1}{2},\frac{1}{2}]$ unless otherwise indicated. Here the elliptic gamma function[5] is defined by the infinite product formula [35],

$$\Gamma_{\mathrm{e}}(z;\sigma,\tau) = \prod_{j,k=0}^{\infty} \frac{1-\mathbf{e}\left(-z+\sigma(j+1)+\tau(k+1)\right)}{1-\mathbf{e}(z+\sigma j+\tau k)}\,. \tag{2.15}$$

The interpretation of the various pieces in (2.14) in its derivation using supersymmetric localization of the partition function [4] are as follows. The gauge holonomies u_i label the localization manifold, and the classical action vanishes at any point on this manifold. The infinite products in the integrand comes from the one-loop determinant of the localization action. The first elliptic gamma function arises from the vector multiplet which has R-charge 2, and the other three elliptic gamma functions arise from the chiral multiplets which carry R-charge $\frac{2}{3}$. The product over i,j in the integrand of (2.16) reflects the fact that all the fields are in the adjoint representation of the gauge group. For the vector multiplets one needs to remove the zero modes which arise for the Cartan elements $i=j$

[5] See [35–37] for a development of the theory and a discussion of the properties of this function.

JHEP09(2020)184

for the vector field, and the non-zero modes of the Cartan elements form the pre-factor in front of the integral (2.14).

In the rest of the paper we analyze the model with $\sigma = \tau$ and $n_0 = -1$ so that the SYM index is

$$\mathcal{I}(\tau) = q^{-\frac{N}{12}}\,\eta(\tau)^{2N}\int[D\underline{u}]\prod_{i\neq j}\Gamma_{\rm e}\big(u_{ij}+2\tau;\tau,\tau\big)\prod_{i,j}\Gamma_{\rm e}\left(u_{ij}+\frac{1}{3}(2\tau+1);\tau,\tau\right)^3 . \quad (2.16)$$

The product expression (2.15) makes it clear that $\Gamma_{\rm e}(z;\tau,\sigma)$ is separately periodic under the translations $z \to z+1$, $\sigma \to \sigma+1$, and $\tau \to \tau+1$. Thus we see from (2.16) that the $\mathcal{N}=4$ SYM index $\mathcal{I}(\tau)$ manifestly has the symmetry $\tau \mapsto \tau+3$. It is also clear from (2.16) that by shifting τ by 1 and 2, respectively, we reach the other two independent values of n_0, thus explicitly showing the relation of n_0 with the contour of integration.

Our goal now is to find complex saddle-points of the integral (2.16). In order to do this we need to extend the integrand to the complex u-plane. One natural guess would be to use analytic continuation of the elliptic gamma function [35]. This function is periodic with period 1, and is almost — but not quite — periodic[6] with period τ: it obeys

$$\frac{\Gamma_{\rm e}(z+\tau;\tau,\tau)}{\Gamma_{\rm e}(z;\tau,\tau)} = \theta_0(z;\tau)\,, \quad (2.17)$$

where the function θ_0 is related to the odd Jacobi theta function ϑ_1 as

$$\theta_0(z;\tau) \coloneqq -\zeta^{\frac{1}{2}}\,q^{\frac{1}{24}}\,\frac{\vartheta_1(\tau,z)}{\eta(\tau)}\,. \quad (2.18)$$

In order to use the method of the previous subsection we need a strictly periodic function, and so we need to find a periodic extension.

Our idea is simple in principle — we deform the integrand away from the real axis such that the resulting function is periodic with period τ. Of course the result will not be meromorphic in u and the best we can hope for a real-analytic function of $\mathrm{Re}(u)$, $\mathrm{Im}(u)$. (We still demand that the action is meromorphic in τ.) The technical goal is thus to replace the integrand of (2.16) by a function that

(a) is periodic under $u \mapsto u + m\tau + n$, $m,n \in \mathbb{Z}$ (an *elliptic function*),

(b) is real-analytic (apart from perhaps a finite number of points on the torus), and

(c) reduces to the product of elliptic gamma functions in (2.16) when $u \in \mathbb{R}$.

The properties (*a*)–(*c*) above do not uniquely fix such a function. We will make a particular choice which has three nice properties. Firstly, our extended action turns out to be closely related to the elliptic dilogarithm function which has, quite remarkably, modular properties under the $SL_2(\mathbb{Z})$ action on τ. As mentioned in the introduction, these properties are made

[6] As we review below, the quasi-periodicity of the $\Gamma_{\rm e}$-function is similar to that of the Jacobi ϑ-functions. Relatedly, it admits an interpretation as "higher degree automorphic forms" [35], but we will not use this cohomological interpretation here.

JHEP09(2020)184

manifest by a formula of Bloch [24], which allows us to calculate the saddle-point action in one simple step. Secondly, the action of the black hole configuration agrees precisely with the supergravity action of the black hole. The third property looks to be an aesthetic or mathematical one at the moment — the elliptic dilogarithm obeys interesting equations, and its values at special points are interesting from a number-theoretic point of view.

We present the details of the extension of the action to the torus in section 3, and continue for now by assuming that there is an extension obeying Properties (a)–(c). The periodicity of the extension under translations of the lattice $\Lambda_\tau = \mathbb{Z}\tau + \mathbb{Z}$ can be restated as saying that the function is well-defined on the torus $\mathbb{C}/\Lambda_\tau$. Now, our lemma about complex saddle-points in the previous subsection means that there is one saddle-point for every lattice point in $\mathbb{Z}\tau + \mathbb{Z}$. If we think of the uniform distribution of eigenvalues $u(x)$ as a string, then a solution corresponding to the point $m\tau + n$ can be thought of as a closed string that winds (m, n) times along the (A, B) cycles of the torus. In terms of the original matrix model, the eigenvalues have moved off the original circle of unit radius into the complex plane, as shown in figure 1.

Comment about other discrete saddles and gcd condition

In the context of our solution-generating lemma in section 2.1, suppose $V(x)$ has *minimal* period T. Then clearly the (discrete) uniform distribution spread between 0 and pT, for any non-zero $p \in \mathbb{Z}$ also solves the saddle-point equations by the same arguments as those given in the lemma. These solutions all give rise to the same distribution of points on the torus if and only if $\gcd(p, N) = 1$. When $(p, N) = (dp', dK)$ with $d > 1$ and $\gcd(p', K) = 1$, then we have a new solution which is a uniform distribution of K "stacks" of eigenvalues, each stack containing $d = \frac{N}{K}$ eigenvalues.

Applying these considerations to our problem on the torus, we find a family of saddles that is classified by the following three-label notation: $(K|\, m, n)$ with $\gcd(m, n) = 1$ and K is a divisor of N. The $m\tau + n$ saddles discussed above correspond to $K = N$, and we will continue to use that notation in that case. If N is prime, saddles are essentially isomorphic to lattice points (m, n) with $\gcd(m, n) = 1$.[7] The one solution which needs to be discussed separately is $(1|\, m, n) \equiv (0, 0)$. This saddle corresponds to the distribution where all eigenvalues are placed at the origin $u = 0$. As we discuss at the end of section E, this distribution of eigenvalues is highly suppressed with respect to the dominant one at finite values of τ. However, one has to be careful to take the limit $\tau \to 0$ because other effects start to appear. From now on, we focus on $(N|\, m, n) \equiv (m, n)$ saddles.

3 Extension of the action to the torus

In this section we show how to extend the matrix model to the torus using elliptic functions. We collect the definitions and properties of some standard functions that appear in our presentation in appendix A.

[7] The relation of these saddles to the Bethe-ansatz configurations will be discussed in appendix F.

JHEP09(2020)184

3.1 Elliptic functions, Jacobi products, and the elliptic dilogarithm

In order to define our deformation, and as a warm-up, we begin with a brief discussion of the quasi-elliptic function $\theta_0(z) = \theta_0(z;\tau)$ defined in equation (2.18). It has the following periodicity properties,

$$\theta_0(z) = \theta_0(z+1) = -\mathbf{e}(z)\,\theta_0(z+\tau)\,, \tag{3.1}$$

and a product representation which follows from the Jacobi product formula,

$$\theta_0(z;\tau) = (1-\zeta)\prod_{n=1}^{\infty}(1-q^n\zeta)\,(1-q^n\zeta^{-1})\,. \tag{3.2}$$

The function θ_0 can be modified slightly in order to obtain a function that is elliptic. Define the related function (recall $z = z_1 + \tau z_2$)

$$P(z) = P(z;\tau) = \mathbf{e}(\alpha_P(z))\,q^{\frac{1}{2}B_2(z_2)}\,\theta_0(z;\tau)\,, \tag{3.3}$$

where B_2 is the second Bernoulli polynomial $B_2(x) = x^2 - x + \frac{1}{6}$. Here the function α_P is chosen to obey

$$\alpha_P(z) \in \mathbb{R}\,, \qquad \alpha_P(z) = 0 \text{ when } z_2 = 0\,, \tag{3.4}$$

and will be specified below.

It is easy to check that the function $q^{-\frac{1}{12}}P(z)$ agrees with $\theta_0(z)$ on the real axis, i.e.,

$$q^{-\frac{1}{12}}P(z;\tau) = \theta_0(z;\tau) \quad \text{when } z_2 = 0\,. \tag{3.5}$$

The elliptic transformations $z \to z+1$, $z \to z+\tau$ are simply shifts of the real variables $z_1 \to z_1+1$, $z_2 \to z_2+1$, respectively. Under $z \to z+1$, the absolute value of each factor in (3.3), and therefore $|P|$, is invariant. Under $z \to z+\tau$, the shift of the theta function (equation (3.1)) is cancelled by the corresponding shift of B_2 (equation (A.6)). Therefore $|P|$ is a doubly periodic function. The phase α_P is chosen so that P itself is doubly periodic. This criterion fixes α_P in terms of θ_0 up to an additive ambiguity of a periodic real function. This ambiguity can be fixed by making a particular choice for α_P, for example, by defining it[8] be to zero in the first fundamental domain $0 < z_2 < 1$, and extending it by periodicity of P. Defined in this manner, the phase $\alpha_P(z)$ is locally constant in z_2, but exhibits a discontinuity when z_2 hits an integer. We can smoothen this discontinuity over a small range ϵ (for instance we can locally replace the Heaviside step function by $\frac{1}{2}(1+\mathrm{erf}(x))$), which is taken to zero at the end of the calculations. As we explain below, the calculations in the following sections are insensitive to the details of the smoothening.

A non-trivial fact is that $|P|$ is also invariant under the modular transformations $\tau \to \frac{a\tau+b}{c\tau+d}$, $z \to \frac{z}{c\tau+d}$. In other words, it is invariant under the full Jacobi group. These properties are immediately demonstrated by the second Kronecker limit formula [27],

$$-\log|P(z;\tau)| = \lim_{s\to 1}\frac{\tau_2^s}{2\pi}\sum_{\substack{m,n\in\mathbb{Z}\\(m,n)\neq(0,0)}}\frac{\mathbf{e}(nz_2 - mz_1)}{|m\tau+n|^{2s}}\,. \tag{3.6}$$

[8] This is equivalent to defining P to be $q^{\frac{1}{2}B_2(\{z_2\})}\,\theta_0(z_1+\{z_2\}\tau;\tau)$.

The right-hand side of (3.6) is a real-analytic Kronecker-Eisenstein series which is manifestly invariant under the Jacobi group.

These properties of θ_0 and P are classical facts known for over a century (see [27] for a beautiful exposition). Interestingly there is a similar story for the elliptic gamma function, which is much more recent. Following [26, 38], we construct the function, for $z \in \mathbb{C}$,

$$Q(z) = Q(z;\tau) = \mathbf{e}(\alpha_Q(z))\, q^{\frac{1}{3}B_3(z_2)-\frac{1}{2}z_2 B_2(z_2)}\, \frac{P(z;\tau)^{z_2}}{\Gamma_{\mathrm{e}}(z+\tau;\tau,\tau)}\,, \tag{3.7}$$

where B_3 is the third Bernoulli polynomial $B_3(x) = x^3 - \frac{3}{2}x^2 + \frac{1}{2}x$. Here we have introduced the phase function α_Q obeying the properties

$$\alpha_Q(z) \in \mathbb{R}\,, \qquad \alpha_Q(z) = 0 \quad \text{when } z_2 = 0\,, \tag{3.8}$$

which we discuss more below. It is easy to check that Q agrees with the Γ_{e}-function on the real axis, i.e.,

$$Q(z;\tau) = \Gamma_{\mathrm{e}}(z+\tau;\tau,\tau)^{-1} \quad \text{when } z_2 = 0\,. \tag{3.9}$$

The quasi-periodicity relation of the elliptic Gamma-function

$$\Gamma_{\mathrm{e}}(z;\tau,\tau) = \Gamma_{\mathrm{e}}(z+1;\tau,\tau) = \theta_0(z;\tau)^{-1}\,\Gamma_{\mathrm{e}}(z+\tau;\tau,\tau) \tag{3.10}$$

implies that the function $|Q|$ is periodic under translations of the lattice $\mathbb{Z}\tau + \mathbb{Z}$.

Remarkably, the function $|Q|$ also satisfies a relation similar to, but more complicated than, the Kronecker limit formula (3.6) for $|P|$. To see the relation, one first notices that the function $|Q|$ is very closely related to the Bloch-Wigner elliptic dilogarithm. The Bloch-Wigner dilogarithm function is the single-valued non-holomorphic function (we follow the treatment of [25]),

$$D(x) \coloneqq \mathrm{Im}(\mathrm{Li}_2(x)) + \arg(1-x)\,\log|x|\,. \tag{3.11}$$

Its elliptic average, which is manifestly invariant under lattice translations, is defined as

$$D(q,x) \coloneqq \sum_{\ell\in\mathbb{Z}} D(q^\ell x)\,. \tag{3.12}$$

The function $D(q,x)$ turns out to have a natural imaginary partner

$$J(q,x) \coloneqq \sum_{\ell=0}^{\infty} J(q^\ell x) - \sum_{\ell=1}^{\infty} J(q^\ell x^{-1}) + \frac{1}{2}\log^2|q|\, B_3\left(\frac{\log|x|}{\log|q|}\right), \tag{3.13}$$

which is itself an elliptic average[9] of the function

$$J(x) \coloneqq \log|x|\,\log|1-x|\,, \tag{3.14}$$

so that the most elegant formulas are written in terms of the combination

$$F(z;\tau) \coloneqq \frac{1}{2\pi}\big(D(q,\zeta) + \mathrm{i}\,J(q,\zeta)\big)\,. \tag{3.15}$$

[9]The definition of $J(q,x)$ is a little more complicated than that of $D(q,x)$ because the function $J(x)$ does not decay as rapidly as $D(x)$ and consequently one needs to regulate the infinite sum.

JHEP09(2020)184

The relation of $|Q|$ to F is as follows [26, 38]

$$\log\left|Q\Big(\frac{z}{\tau};-\frac{1}{\tau}\Big)\right|-\tau\log|Q(z;\tau)|=F(z;\tau)\,. \tag{3.16}$$

The relation to Kronecker-Eisenstein series follows from the following formula [24, 25],

$$F(z;\tau)=\frac{\tau_2^2}{2\pi^2}\sum_{\substack{m,n\in\mathbb{Z}\\(m,n)\neq(0,0)}}\frac{\mathbf{e}(nz_2-mz_1)}{(m\tau+n)(m\overline{\tau}+n)^2}\,. \tag{3.17}$$

The function F is manifestly invariant under shifts of u by lattice points. The form of $F(\tau,z)$ as a lattice sum also makes it clear that under modular transformations

$$\tau\mapsto\frac{a\tau+b}{c\tau+d}\,,\qquad z\mapsto\frac{z}{c\tau+d}\,,\qquad \begin{pmatrix}a&b\\c&d\end{pmatrix}\in SL_2(\mathbb{Z})\,, \tag{3.18}$$

it transforms as a Jacobi form of weight $(0,1)$. The real and imaginary parts of equation (3.16) give us formulas for $\log|Q|$ as well as its modular transform in terms of the real and imaginary parts of F,

$$-\tau_2\log|Q(z;\tau)|=\frac{1}{2\pi}J(q;\zeta)\,,\quad \log\left|Q\Big(\frac{z}{\tau};-\frac{1}{\tau}\Big)\right|=\frac{1}{2\pi}\left(D(q;\zeta)+\frac{\tau_1}{\tau_2}J(q;\zeta)\right), \tag{3.19}$$

for which we can write Fourier expansions using the expansion (3.17).

The above discussion completely defines the function $\log|Q|=\operatorname{Re}\log Q$, but the phase function α_Q, and therefore $\operatorname{Im}\log Q$, still needs to be defined properly.[10] We want to choose the phase α_Q such that the whole function Q is doubly periodic. As in the case of P, this criterion determines α_Q in terms of the function Γ_e up to an additive ambiguity of a periodic real function. Unlike in the case of P, we do not fix this ambiguity completely yet. Instead, we write $\alpha_Q(z)=\alpha_Q^0(z)+\Psi_Q(z)$ where α_Q^0 is fixed by a particular choice, e.g. by demanding that it vanishes in the first fundamental region and extending it by demanding periodicity of Q.[11] We have explicitly parameterized the ambiguity by a doubly-periodic real function $\Psi_Q(z)$ which vanishes at $z_2=0$, which we fix in section 3.3.

Alternatively, we can define $\operatorname{Im}\log Q$ to be the harmonic dual of $\operatorname{Re}\log Q$ with respect to τ. In other words we construct $\log Q$ by demanding that it is holomorphic in τ and has the same real part as $\operatorname{Re}\log Q$. Using the relations (3.19), (3.15), and the Fourier expansion (3.17), we can write a Fourier expansion for $\log Q$ as follows,

$$\begin{aligned}\log Q(z;\tau)&=-\frac{1}{4\pi^2}\sum_{\substack{m,n\in\mathbb{Z}\\m\neq0}}\frac{\mathbf{e}(nz_2-mz_1)}{m(m\tau+n)^2}+\frac{\tau}{2\pi^2}\sum_{\substack{n\in\mathbb{Z}\\n\neq0}}\frac{\mathbf{e}(nz_2)}{n^3}+\frac{\pi\mathrm{i}}{4}\sum_{\substack{m,n\in\mathbb{Z}\\m\neq0}}K(m,n)\,\mathbf{e}(nz_2-mz_1)\,,\\&=-\frac{1}{4\pi^2}\sum_{\substack{m,n\in\mathbb{Z}\\m\neq0}}\frac{\mathbf{e}(nz_2-mz_1)}{m(m\tau+n)^2}+\frac{2\pi\mathrm{i}\tau}{3}B_3\big(\{z_2\}\big)+\pi\mathrm{i}\,\Psi(z)\,.\end{aligned} \tag{3.20}$$

[10] The function Q should be related to a version of the elliptic dilogarithm holomorphic in τ studied in [39, 40], we leave a detailed study of this to the future.

[11] This choice leads to the value $\alpha_Q^0(z)=-\frac{1}{4}(1+2\{z_1\})\,\lfloor z_2\rfloor\,(1+\lfloor z_2\rfloor)$.

JHEP09(2020)184

In defining the harmonic dual there is an additive ambiguity in $\operatorname{Im}\log Q$ of a τ-independent doubly periodic real function, which we have denoted by $\Psi(z)$, and whose Fourier coefficients we have denoted by $\frac{1}{4}K(m,n)$. By comparing the expression (3.20) to the expansion (C.3) of $\Gamma_{\rm e}$, and using the constraint (3.9), we obtain that $\Psi(z)|_{z_2=0}=0$. The ambiguity Ψ in the Fourier expansion is in one-to-one correspondence with the ambiguity Ψ_Q in the definition (3.7) which we discussed in the previous paragraph. The difference $\Psi(z)-\Psi_Q(z)$ is an unambiguous doubly periodic function which we do not calculate here.

The function $\operatorname{Im}\log Q$ as defined above is not smooth, in particular, it is continuous but its first derivative is discontinuous at integer values of z_2. We can smoothen this discontinuity, as we did for $\log P$, over a small range ϵ. In the following sections we apply the lemma in section 2.1 to potentials which are linear combinations of $\log P$ and $\log Q$. The first part of the lemma states that periodic configurations of eigenvalues solve the saddle point equations for smooth periodic functions, this part clearly goes through in a straightforward manner for the smoothened functions. The second part of the lemma states that the action of the periodic configurations is the zeroth Fourier coefficient of the potential V. Here, we note that the region of smoothening, and therefore the contribution of the integrals of $\log P$ and $\log Q$ from the region near the discontinuities, vanishes as $\epsilon\to 0$ (note that there is no derivative acting on V in the calculation of the action). In other words, the zeroth Fourier coefficients of the smoothened functions $\log P$ and $\log Q$ can still be calculated from the Fourier expansions (3.6), (3.17), and (3.20).

3.2 Elliptic extension of the action

Having set up the basic formalism, we can now connect to the action of $\mathcal{N}=4$ SYM. In order to do so, we define the related function

$$Q_{a,b}(z)=Q_{a,b}(z;\tau)\coloneqq q^{\frac{a^3}{6}-\frac{a}{12}}\,\frac{Q(z+a\tau+b)}{P(z+a\tau+b)^a}\,,\qquad a,b\in\mathbb{R}\,. \tag{3.21}$$

This function is doubly periodic since all its building blocks are, and it obeys the property

$$Q_{a,b}(z)=\Gamma_{\rm e}(z+(a+1)\tau+b;\tau,\tau)^{-1}\quad\text{when } z_2=0\,. \tag{3.22}$$

The index (2.16) can now be written as

$$\mathcal{I}(\tau)=\big(q^{-\frac{1}{24}}\eta(\tau)\big)^{2N}\int[D\underline{u}]\prod_{i\neq j}Q_{1,0}(u_{ij})^{-1}\prod_{i,j}Q_{-\frac{1}{3},\frac{1}{3}}(u_{ij})^{-3}\,. \tag{3.23}$$

We can write this in terms of an effective action as

$$\mathcal{I}(\tau)=\int[D\underline{u}]\,\exp(-S(\underline{u}))\,, \tag{3.24}$$

with

$$S(\underline{u})=-2N\log\big(q^{-1/24}\,\eta(\tau)\big)+\sum_{i\neq j}\log Q_{1,0}(u_{ij})+3\sum_{i,j}\log Q_{-\frac{1}{3},\frac{1}{3}}(u_{ij})\,. \tag{3.25}$$

JHEP09(2020)184

In terms of the functions Q and P we have

$$\begin{aligned} S(\underline{u}) = &-2N\log\big(q^{-1/24}\,\eta(\tau)\big) - \frac{1}{6}N\pi\mathrm{i}\tau + \frac{8}{27}\pi\mathrm{i}\tau N^2 \\ &+ \sum_{i\neq j}\log Q\big(u_{ij}+\tau\big) + 3\sum_{i,j}\log Q\big(u_{ij}-\tfrac{1}{3}\tau+\tfrac{1}{3}\big) \\ &- \sum_{i\neq j}\log P\big(u_{ij}+\tau\big) + \sum_{i,j}\log P\big(u_{ij}-\tfrac{1}{3}\tau+\tfrac{1}{3}\big)\,. \end{aligned} \tag{3.26}$$

We have thus reached our goal of extending the action to the complex plane in terms of doubly periodic functions. The action is a real-analytic function on the torus except for a finite number of points where it has singularities, we comment on this in appendix B.

The fact that the expansions (3.17) and (3.20) are written as a double Fourier series in z_1, z_2 means that we can read off the average value in any desired direction in the z-plane. Secondly this expression in terms of a lattice sum makes the modular properties completely manifest. We will use these properties in the following section to calculate the action at the saddle-points, and to calculate asymptotic formulas in the Cardy-like limit.

3.3 Deforming the contour

We now turn to the evaluation of the integral (3.23). By construction the integrand is a doubly periodic function with periods 1 and τ. Applying the lemma of section 2.1, we conclude that the uniform distribution of the eigenvalues between 0 and the lattice point $m\tau+n$, $m,n\in\mathbb{Z}$ solves the variational equations. However, in order for this configuration to be a genuine saddle-point of the integral, the contour of integration needs to pass through it. The original contour in (3.23) runs over $u_i\in[0,1]$, $i=1,\ldots,N$, while the value of u_i at the saddle (m,n) is

$$u_i = \frac{i}{N}(m\tau+n) \iff u_{ij} = \frac{i-j}{N}(m\tau+n)\,, \tag{3.27}$$

which is not on the original contour.

To our knowledge, two approaches have been followed to deal with this issue in similar problems with meromorphic integrands. The first approach can be seen in the problem of counting black hole microstates in $\mathcal{N}=4$ string theory in asymptotically flat space, wherein the degeneracy of microstates is given by a contour integral of a meromorphic function. In this case one deforms the contour so as to pass through the saddle, and keeps track of any residues that are picked up in the process [41, 42]. The other approach is Picard-Lefschetz theory wherein one constructs a basis of the homology of the manifold (or relative homology for non-compact spaces), and then decomposes a given contour in terms of these basis elements, see e.g. [28, 43]. Since the integrand in our discussion is not meromorphic, we cannot apply either of these methods directly. As we do not know of a rigorous mathematical formalism to approach this problem, we only make some observations in this subsection, and leave a complete analysis of this important issue to future work. In particular, we make two related points, pertaining to the two methods mentioned above.

JHEP09(2020)184

The first point is that there is a close relation between the doubly periodic integrand (3.23) that is our focus, and the meromorphic integrand of (2.16). As we saw in the previous subsection, these two integrands are equal to each other when all the u_i are real because of the identity (3.22). In fact, as we show below, they are also equal to each other when evaluated on the saddle-point configuration (3.27). Thus, one way to deal with the contour deformation could be to apply the Picard-Lefschetz theory to the meromorphic integrand, and use its equality to the doubly-periodic integrand on the saddles at the end of the process.[12]

In order to show this equality we first note that, as a direct consequence of the definitions of the various functions, we can write, for all z,

$$Q_{a,b}(z) = e^{2\pi \mathrm{i}(\Psi_Q(z+a\tau+b)+\alpha_Q^0(z+a\tau+b))}\, q^{-A_a(z_2)}\, \frac{P(z+(a+1)\tau+b;\tau)^{z_2}}{\Gamma_{\mathrm{e}}(z+(a+1)\tau+b;\tau,\tau)}\,, \tag{3.28}$$

where the cubic polynomial A_a is defined as

$$A_a(x) = \tfrac{1}{6}\,x^3 + \tfrac{1}{2}a\,x^2 + \left(\tfrac{1}{2}a^2 - \tfrac{1}{12}\right)x\,. \tag{3.29}$$

Now, the integrands of (3.23) and (2.16) involve a product over $a = 1, -\frac{1}{3}, -\frac{1}{3}, -\frac{1}{3}$ (from the product over vector and chiral multiplets), and over all pairs (i,j). The fact that we sum over the pairs (i,j) and (j,i) for a given i,j means that only the quadratic term in the above polynomial survives in the full integrand. This term is proportional to a, which vanishes after summing over the four values that it takes. Thus the contribution of the cubic polynomial A_a to the integrand vanishes. The contribution of the function $|P|$ to the integrand can be written as the exponential of

$$\sum_{i,j=1}^{N} (u_{ij})_2 \left(\log\left|P\big(u_{ij}+2\tau+1\big)\right| + 3\log\left|P\big(u_{ij}+\tfrac{2}{3}\,(2\tau+1)\big)\right|\right). \tag{3.30}$$

We can evaluate this expression on the saddle point $u_i = \frac{i}{N}(m\tau+n)$ using the double Fourier expansion (3.6) for the function $\log|P|$. In this manner we obtain a sum over the integers $\widetilde{n}, \widetilde{m}$ of two terms corresponding to the two terms in (3.30). Now, each term contains the factor

$$\sum_{i,j=1}^{N} (i-j)\,\mathbf{e}\big(\tfrac{i-j}{N}(\widetilde{n}m - \widetilde{m}n)\big)\,, \tag{3.31}$$

which actually vanishes, as proved in equation (E.6).[13] Thus we reach the conclusion that the integrands of (3.23) and (2.16) are equal in magnitude on the saddle point configurations. We had left the phase $\Psi_Q(z)$ ambiguous until now, and we fix it by demanding that

[12] Another possibility, suggested by a referee whom we thank, is to use real-harmonic functions. We have not been able to make this interesting suggestion more precise.

[13] The fact that the full function P is doubly periodic implies that it has a double Fourier expansion similar to (3.6). The identity (3.31) then also implies that the contribution of P to the action also vanishes.

JHEP09(2020)184

the phases of the two integrands are also equal at each saddle point.[14] In appendix E we have another proof of the equality of the two forms of the action using a series representation of the various functions.

The second point is the construction of a new contour that passes through the saddle-point, and the associated analysis of the effect of the change in contour. The new contour $\mathcal{C}$ of integration for the integral (3.23) is constructed as follows. In each u_k-plane, we cut a small interval from the real axis of width ε (which we eventually take to zero), and lying directly below the saddle-point value $u_k = \frac{k}{N}(m\tau + n)$, and parallel transport it upwards so that it goes through the saddle point value. Then we complete the contour by adding two vertical lines with opposite orientation. The new contour $\mathcal{C}$ is the sum of the original contour $[0, 1]$ and the closed contour D_k in each u_k-plane. This is shown in figure 2. We now want to calculate the change in the value of the integral (3.23) when we change the contour from $[0, 1]^N$ to $\mathcal{C}$ as $N \to \infty$, or, equivalently, the sum of the integrals around the closed contour D_k. The assertion is that we can essentially replace the integrand of (3.23) by the meromorphic integrand of (2.16) everywhere along D_k, which we can calculate using the method of residues.

How do we justify the replacement? On the bottom horizontal piece of D_k this is because of the equality (3.22). The two vertical sides have opposite orientations and therefore cancel out as $\varepsilon \to 0$. In this limit of vanishing width, we can also replace the integrand of (2.16) by the integrand of (3.23) on the top horizontal part of the contour as we argued above. Having reached the contour $\mathcal{C}$ we can now use the saddle-point approximation to calculate the integral. There is one point in this argument where we have to be careful. On the one hand, we want $\varepsilon \to 0$ so that the replacement of the doubly periodic integrand by the meromorphic integrand on the top strip is a good approximation. On the other hand, we recall that in the saddle-point method we essentially approximate the function by a Gaussian near its saddle, and most of the value of the integral comes from a region close to the saddle-point. In order for the method to be valid we should not take $\varepsilon \to 0$ too fast. In our case the large factor in front of the exponent for each eigenvalue is N, and so if we take $\varepsilon = \frac{1}{\sqrt{N}}$ we safely pick up most of the value of the Gaussian.

We can now check that the error caused by the replacement on the interval at the top of D_k is sub-leading in N. The configuration $u_k = \frac{k}{N}(m\tau + n)$ is a saddle-point for the doubly periodic action and we can use the Gaussian formula including the first subleading term to estimate the integral along the top interval. On the other hand it is regular point for the meromorphic action and the value of its integral along the top interval is the value

[14] Here a question arises as to whether this prescription for Ψ_Q is well-defined. In particular, it could happen that a certain point z on the torus lies on the string of eigenvalues for two different saddles (m, n) and (m', n'). The point z would correspondingly lift to two different points in the complex plane which differ by a lattice translation. The question then is whether the value of the phase of Γ_e and in particular the value of α_Q^0 agrees at these two points. This is a subtle question whose complete analysis will be posted elsewhere. For our purposes here, we restrict our analysis to a set of saddles with an upper cutoff on m. In this situation if we take α_Q^0 to be defined as in Footnote 11, the difference in α_Q^0 between two points differing by a lattice translation is a rational number with a bounded denominator. We can then lift our discussion to a larger torus (which is still finite) on which Ψ_Q is well-defined. We note that all the calculations of the action are done by considering points on the complex plane, so that they are not affected by this cutoff.

JHEP09(2020)184

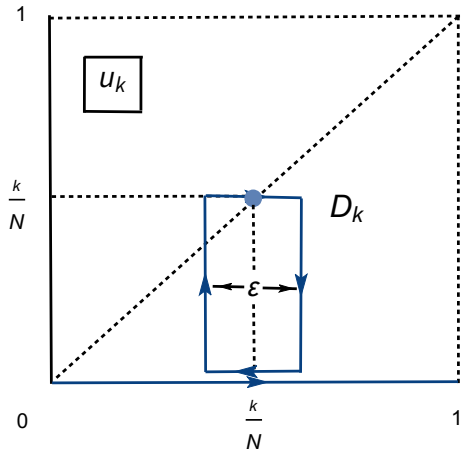

Figure 2. The new contour of integration that passes through the saddle-point is the sum of the contour along $[0,1]$ and the closed contour D_k in each coordinate u_k. The figure shows the u_k plane for one k with the axes denoting the two components of u_k (decomposed in our notation $z = z_1 + \tau z_2$) running from 0 to 1 so as to cover the fundamental parallelogram.

at the saddle point multiplied by ε up to an order one constant. Thus, the ratio of the two integrals on the top strip equals $a \times \varepsilon\sqrt{N} = a$, where a is an order one constant, for each variable, so that the total error in the full effective action is $N \log a$. In the next section we estimate the saddle-point value of the action and we find that for an infinite family of saddles, including the black hole saddle, the action is proportional to N^2. For these saddles the error term $N \log a$ is a sub-leading contribution. Thus we reach the conclusion that the change in the integral (3.23) upon deforming the contour from $[0,1]^N$ to $\mathcal{C}$ as $N \to \infty$ equals the sum of the residues of the integrand of (2.16) inside the various D_k. We postpone a complete analysis of the contours and residues to the future.

Upon putting together the two observations above, we reach the conclusion that the (m,n) solutions to the variational equations are genuine saddle-point configurations contributing to the integral expression for the index. We emphasize again that the above discussion only applies locally near the saddles, i.e. it only shows that the contour can pass through the saddle-point. In particular, it does not tell us what the exact contour is, and a rigorous global analysis of the contour remains to be done. We proceed by writing the full integral as a sum over the various saddles (or phases) with an effective action at each saddle. This sum should be regarded in the same sense as the sum over instantons in quantum field theory and, in particular, we do not treat issues of convergence. We are, however, in a position to compare the effective actions at the various saddles and find the phase structure of the theory at leading order in the large-N approximation. In the following section we calculate this effective action and the consequent phase structure.

4 Action of the saddles, black holes, and the phase structure

The considerations of the previous two sections have shown that the complex saddles for the supersymmetric index (2.16) of $\mathcal{N} = 4$ SYM on $S^3 \times S^1$ in the large-N limit are labelled

JHEP09(2020)184

by the lattice points $m\tau + n \in \mathbb{Z}\tau + \mathbb{Z}$ with $\gcd(m,n) = 1$.[15] After taking into account the caveats in the discussion of section 3.3, we can write the index as a sum over saddles as follows

$$\mathcal{I}(\tau) \sim \sum_{\substack{m,n\in\mathbb{Z} \\ \gcd(m,n)=1}} \exp\bigl(-S_{\text{eff}}(m,n;\tau)\bigr)\,. \tag{4.1}$$

The effective action $S_{\text{eff}}(m,n;\tau)$ is the classical action (3.25) evaluated at the saddle-point configuration (m,n) plus the quantum corrections induced by loop effects around the saddle. In this paper we only calculate the classical part. In this section we show that the action of the $(1,0)$ saddle agrees with that of the supersymmetric black hole in the dual AdS_5 theory. We then compare the real parts of the actions at the different saddle-points as a function of τ which leads to the phase structure of the theory.

4.1 Action of the saddles

In the large-N limit the effective action (3.25) of the SYM theory extended to the torus can be written in terms of a potential as in (2.4),

$$\begin{aligned} V(z) &= \log Q_{1,0}(z) + 3\log Q_{-\frac{1}{3},\frac{1}{3}}(z) \\ &= \frac{8}{27}\pi\mathrm{i}\tau + \log Q\bigl(z+\tau\bigr) + 3\log Q\bigl(z-\tfrac{1}{3}\tau+\tfrac{1}{3}\bigr) - \log P\bigl(z+\tau\bigr) + \log P\bigl(z-\tfrac{1}{3}\tau+\tfrac{1}{3}\bigr)\,. \end{aligned} \tag{4.2}$$

The formula (2.8) says that the value of the action at the saddle-point $m\tau + n$ is given by the average value of the action (as a function of z) on the straight line between the origin and that point. In terms of the coefficients of the double Fourier series

$$V(z) = \sum_{m,n\in\mathbb{Z}} \mathbf{e}(nz_2 - mz_1)\, V_{m,n}\,, \tag{4.3}$$

the average value of V between 0 and $m\tau + n$ ($\gcd(m,n) = 1$) is

$$\int_0^1 dx\, V(x(m\tau+n)) = \sum_{m',n'\in\mathbb{Z}} V_{m',n'} \int_0^1 dx\, \mathbf{e}\bigl((n'm - m'n)x\bigr) = \sum_{p\in\mathbb{Z}} V_{pm,pn}\,. \tag{4.4}$$

Here in the second equality we have used that the integral of $\int_0^1 \mathbf{e}(nx)dx = \delta_{n,0}$.

We will now use the formula (4.4) to calculate the average value of the action. In preparation for the result we first calculate the average values of the functions $\log P$ and $\log Q$. As discussed below equation (3.19), it is easier to calculate the average value of the real parts $\log|P|$ and $\log|Q|$. To reach the complex function we construct an expression holomorphic in τ whose real part agrees with these calculations. (We only present that after having assembled the full action, but it is easy to do this at every step if required.) This still leaves the ambiguity of a τ-independent purely imaginary term, we shall discuss this in the context of the $(1,0)$ saddle in detail in the following subsection, and more generally in appendix E.

[15] The expressions in the rest of this section are valid for points obeying the condition $\gcd(m,n) = 1$.

JHEP09(2020)184

Average value of $\log|P|$. The double Fourier series given by the Kronecker limit formula (3.6) implies that, for $(m,n)\neq(0,0)$,

$$\begin{aligned}\int_0^1 dx\,\log\left|P\big(x(m\tau+n)+a\tau+b\big)\right| &= -\frac{\tau_2}{2\pi}\,\frac{1}{|m\tau+n|^2}\sum_{\substack{p\in\mathbb{Z}\\ p\neq 0}}\frac{1}{p^2}\,\mathbf{e}\big((na-mb)p\big)\\ &= -\pi\tau_2\,\frac{1}{|m\tau+n|^2}\,B_2\big(\{mb-na\}\big)\,.\end{aligned}\tag{4.5}$$

Average value of $\log|Q|$. The double Fourier series given by the Bloch formula (3.17) implies that, for $(m,n)\neq(0,0)$,

$$\begin{aligned}\int_0^1 dx\,\log\left|Q\big(x(m\tau+n)+a\tau+b\big)\right| &= \mathrm{i}\,\frac{\tau_2}{2\pi^2}\,\frac{(m\tau_1+n)}{|m\tau+n|^4}\sum_{\substack{p\in\mathbb{Z}\\ p\neq 0}}\frac{1}{p^3}\,\mathbf{e}\big((na-mb)p\big)\\ &= \frac{2}{3}\pi\tau_2\,\frac{(m\tau_1+n)}{|m\tau+n|^4}\,B_3\big(\{mb-na\}\big)\,.\end{aligned}\tag{4.6}$$

In reaching the second lines in the above formulas we have used the Fourier expansions (A.8), (A.9) for the Bernoulli polynomials.

Average value of $\log|Q_{ab}|$. Putting these two together we can calculate the average value of $\log Q_{ab}$ to be

$$\begin{aligned}&\int_0^1 dx\,\log\left|Q_{ab}\big(x(m\tau+n)\big)\right| = \\ &= \pi\tau_2\left(\frac{a(1-2a^2)}{6}+\frac{2}{3}\,\frac{(m\tau_1+n)}{|m\tau+n|^4}\,B_3\big(\{mb-na\}\big)+a\,\frac{1}{|m\tau+n|^2}\,B_2\big(\{mb-na\}\big)\right).\end{aligned}\tag{4.7}$$

Vector multiplet action. The real part of the vector multiplet contribution to the saddle-point action is given by

$$\begin{aligned}\mathrm{Re}\,S^{\mathrm{vec}}_{\mathrm{eff}}(m,n;\tau) &= N^2\int_0^1 dx\,\log\left|Q_{1,0}\big(x(m\tau+n)\big)\right|\\ &= N^2\pi\tau_2\left(-\frac{1}{6}+\frac{2}{3}\,\frac{(m\tau_1+n)}{|m\tau+n|^4}\,B_3(0)+\frac{1}{m(m\tau+n)}\,B_2(0)\right),\\ &= N^2\pi\tau_2\left(-\frac{1}{6}+\frac{1}{6}\,\frac{1}{|m\tau+n|^2}\right).\end{aligned}\tag{4.8}$$

Chiral multiplet action. The real part of the chiral multiplet contribution to the saddle-point action is given by

$$\begin{aligned}&\mathrm{Re}\,S^{\mathrm{chi}}_{\mathrm{eff}}(m,n;\tau)\\ &= N^2\int_0^1 dx\,\log\left|Q_{-\frac{1}{3},\frac{1}{3}}\big(x(m\tau+n)\big)\right|\\ &= N^2\pi\tau_2\left(-\frac{7}{162}+\frac{2}{3}\,\frac{(m\tau_1+n)}{|m\tau+n|^4}\,B_3\big(\{\tfrac{1}{3}(m+n)\}\big)-\frac{1}{3}\,\frac{1}{|m\tau+n|^2}\,B_2\big(\{\tfrac{1}{3}(m+n)\}\big)\right).\end{aligned}\tag{4.9}$$

JHEP09(2020)184

$\ell \pmod 3$	0	1	2
$B_3(\{\frac{\ell}{3}\})$	0	1/27	−1/27
$\frac{1}{6} - B_2(\{\frac{\ell}{3}\})$	0	2/9	2/9

Table 1. The coefficients of the second and third terms in equations (4.10).

χ \ ℓ	0	1	2
χ_0	0	1	1
χ_1	0	1	−1

Table 2. The two Dirichlet characters modulo 3.

$\mathcal{N} = 4$ SYM action. Putting everything together, we reach the following concise formula for the real part of the total action at the (m, n) saddle-point,

$$\begin{aligned}
&\operatorname{Re} S_{\text{eff}}(m,n;\tau) \\
&= \operatorname{Re} S^{\text{vec}}(m,n;\tau) + 3 \operatorname{Re} S^{\text{chi}}(m,n;\tau) \\
&= N^2 \pi \tau_2 \left(-\frac{8}{27} + 2\,\frac{(m\tau_1+n)}{|m\tau+n|^4}\, B_3\big(\{\tfrac{1}{3}(m+n)\}\big) + \frac{1}{|m\tau+n|^2}\left(\frac{1}{6} - B_2\big(\{\tfrac{1}{3}(m+n)\}\big)\right)\right).
\end{aligned} \tag{4.10}$$

The coefficients of the second and third terms in the above formula are periodic in their arguments and take the values given in table 1. The symmetry $\tau \mapsto \tau + 3$ is realized in this formula as $(m, n) \mapsto (m, n + 3m)$. Under this operation the combination $\frac{1}{3}(m + n) \mapsto \frac{1}{3}(m + n) + m$, so that the fractional part of this number in the argument of the Bernoulli polynomials does not change. It is clear from this formula that

$$\operatorname{Re} S_{\text{eff}}(m,n;\tau) = -\frac{8}{27} N^2 \pi \tau_2 \qquad \text{when } m + n = 0 \bmod 3\,. \tag{4.11}$$

Using the values of the Bernoulli polynomials in table 1 we can rewrite the real part of the action as

$$\operatorname{Re} S_{\text{eff}}(m,n;\tau) = \frac{2}{27} N^2 \pi\, \tau_2 \left(-4 + \frac{(m\tau_1+n)}{|m\tau+n|^4}\, \chi_1(m+n) + \frac{1}{|m\tau+n|^2}\, 3\chi_0(m+n) \right), \tag{4.12}$$

where χ_i, $i = 0, 1$ are the two Dirichlet characters of modulus 3 (see table 2).

Upon constructing the holomorphic part of the action as explained above, we obtain $S(0, 1; \tau) = 0$ and a short calculation shows that, for $m \neq 0$,

$$S_{\text{eff}}(m,n;\tau) = \frac{N^2 \pi \mathrm{i}}{27\, m}\, \frac{\big(2(m\tau+n) + \chi_1(m+n)\big)^3}{(m\tau+n)^2} + N^2 \pi \mathrm{i}\, \varphi(m,n)\,, \tag{4.13}$$

where the τ-independent real phase φ is

$$\varphi(m,n) = \widetilde{K}(m,n) - \frac{1}{27}\left(8\frac{n}{m} + \frac{12}{m}\, \chi_1(m+n) \right), \tag{4.14}$$

JHEP09(2020)184

where in terms of the function K in (3.20), we have

$$\widetilde{K}(m,n) = \sum_{p\in\mathbb{Z}} K(pm,pn)\,. \tag{4.15}$$

It is interesting to ask what is the action of a given saddle-point configuration if we use the analytic continuation of the elliptic gamma function instead of the elliptic continuation presented here. We address this question in appendix E and find that the results coincide, up to a τ-independent imaginary constant. The phenomenon that the action of a given saddle essentially does not change if we use the analytic continuation of the elliptic gamma function instead of the elliptic continuation is interesting. At the practical level, the meromorphic analysis of appendix E, can be used to extend the current results of the Bethe ansatz approach of [7, 8] and, to relate those with the results of the elliptic approach introduced here.

4.2 Entropy of supersymmetric $\mathbf{AdS_5}$ black holes

A particularly interesting saddle-point is the black-hole $(m,n)=(1,0)$, whose action is

$$S_{\text{eff}}(1,0;\tau) = \frac{\pi \mathrm{i}\, N^2\,(2\tau+1)^3}{27\,\tau^2} + \pi\mathrm{i}\, N^2 \varphi(1,0)\,. \tag{4.16}$$

Up to a τ-independent additive constant that we discuss below, this action is equal to the action of the supersymmetric AdS_5 black hole, calculated in [4] from supergravity after explicitly solving the constraint (1.2) for φ and subsequently setting $\tau=\sigma$. In [4] the black hole entropy was derived by performing a Legendre transform which includes a Lagrange multiplier that enforces the constraint. Here we verify that one can equivalently obtain the result for the black hole entropy by explicitly solving the constraint. As we see below the Legendre transform of the action (4.16) combined with a set of reality conditions on the expectation values of charges and the entropy leads to the Bekenstein-Hawking entropy of the BPS black hole [3, 4].

The entropy of the black hole comes from the $(1,0)$ saddle-point as

$$\mathrm{e}^{\mathcal{S}_{BH}(Q,\,J)} = \int d\tau\, \exp\big(\mathcal{E}(\tau)\big)\,, \qquad \mathcal{E}(\tau) = -S_{\text{eff}}(1,0;\tau) - 2\pi\mathrm{i}\,\tau\big(2J+Q\big) - \pi\mathrm{i}\,Q\,, \tag{4.17}$$

with $J=\frac{1}{2}(J_1+J_2)$. There are two τ-independent terms in the exponent of the right-hand side which deserve a comment. One is the last term on the right-hand side which appears from a similar term in the Hamiltonian definition of the index (2.9) with $n_0=-1$. The other is the value of the constant $\varphi(1,0)$ that we fix to zero by the choice $\widetilde{K}(1,0)=\frac{12}{27}$ in (4.16), so that

$$S_{\text{eff}}(1,0;\tau) = \frac{\pi\mathrm{i}\,N^2}{27}\frac{(2\,\tau+1)^3}{\tau^2}\,. \tag{4.18}$$

In the large-N regime, the integral (4.17) is approximated by its saddle-point value, and as usual we assume that the integration contour goes through the saddle-point. Thus we have to extremize the functional $\mathcal{E}(\tau)$.

JHEP09(2020)184

We find that, as a result of this extremization procedure, the black hole entropy obeys $P(\frac{\mathrm{i}}{2\pi}\mathcal{S}_{BH}) = 0$, where P is the cubic polynomial

$$\begin{aligned} P(x) &= \Big(-\frac{Q}{2} + x\Big)^3 - \frac{N^2}{2}\big(J + x\big)^2, \\ &\equiv p_0 + p_1\, x + p_2\, x^2 + x^3\,. \end{aligned} \tag{4.19}$$

This is precisely the polynomial that was found to govern the gravitational entropy of the supersymmetric extremal black holes in [4]. In addition if we impose the reality conditions

$$\mathrm{Im}(\mathcal{S}_{BH}) = \mathrm{Im}(J) = \mathrm{Im}(Q) = 0\,, \tag{4.20}$$

we find that the charges J and Q obey the following constraint

$$p_0 = p_1\, p_2\,, \tag{4.21}$$

where

$$p_0 = -N^2\frac{J^2}{2} - \frac{Q^3}{8}\,, \qquad p_1 = \frac{3\,Q^2}{4} - N^2 J\,, \qquad p_2 = -\frac{3Q}{2} - \frac{N^2}{2}\,, \tag{4.22}$$

are the coefficients of P defined in (4.19). With these reality conditions, we obtain the following result for the entropy,

$$\mathcal{S}_{BH} = \pi\sqrt{3Q^2 - 4N^2 J}\,, \tag{4.23}$$

which agrees with the Bekenstein-Hawking entropy of the corresponding BPS black holes. Based on the black hole properties, we shall call the SYM saddle-points with real expectation value of charges and entropy as *extremal*.

The above results can be obtained as follows. Upon extremising $\mathcal{E}(\tau)$ one obtains the following relation

$$2J + Q = -N^2\,\frac{(\tau-1)(2\tau+1)^2}{27\tau^3}\,. \tag{4.24}$$

Plugging this relation into $\mathcal{E}(\tau)$ one obtains, at the saddle point

$$\mathcal{S}_{BH} = \mathcal{E}(\tau) = -\pi\,\mathrm{i}\,N^2\frac{(2\tau+1)^2}{9\tau^2} - \pi\,\mathrm{i}\,Q\,. \tag{4.25}$$

The above two equations imply that the quantity $s = \frac{\mathrm{i}}{2\pi}\mathcal{S}_{BH}$ obeys, at the saddle point,

$$s - \frac{Q}{2} = \frac{N^2}{18}\,\frac{(2\tau+1)^2}{\tau^2}\,, \qquad s + J = \frac{N^2}{54}\,\frac{(2\tau+1)^3}{\tau^3}\,. \tag{4.26}$$

Putting these two equations together we find that $P(s) = 0$.

Upon imposing the reality condition of J and Q in (4.24) we obtain that the extremal solutions lie on the following real one-dimensional locus in the complex τ-plane (we denote the corresponding quantities by *),

$$\tau_2^* = \sqrt{-\frac{3{\tau_1}^2(2\tau_1+1)}{6\tau_1 - 1}}\,. \tag{4.27}$$

JHEP09(2020)184

Now imposing the reality of $\mathcal{S}_{BH}$ and Q in (4.24), (4.25), we obtain

$$J^* = \frac{N^2\,(2\tau_1+1)^2\,(7\tau_1-1)}{432\,{\tau_1}^3}\,, \qquad Q^* = -\,\frac{N^2\,(2\tau_1+1)\,(10\tau_1-1)}{72\,{\tau_1}^2}\,. \tag{4.28}$$

One can now check that the expressions (4.28) satisfy the non linear constraint (4.21), and that the right-hand side of (4.25) equals the expression (4.23). One can ask what happens if we choose differently the τ-independent term $\varphi(1,0)$ in the extremization problem (4.17). This is answered by noticing that without these terms the exponent has the symmetry which shifts J and $\frac{Q}{2}$ equally in opposite directions keeping $2J+Q$ invariant. The actual minimization procedure (e.g. in equation (4.24)) only depends on this combination. However, the reality conditions that we impose break this symmetry. Now it is clear that if we change these terms, e.g. if we change the value of the constant $\widetilde{K} = \widetilde{K}(1,0)$ away from $\frac{12}{27}$, then the whole procedure that we described above still goes through, but with the redefinitions $Q \to Q + N^2(\widetilde{K} - \frac{12}{27})$, $J \to J - \frac{N^2}{2}(\widetilde{K} - \frac{12}{27})$. However, we note that the value of $\widetilde{K} = \frac{12}{27}$ that agrees with the supergravity entropy *function* is precisely the one given by the analytic continuation of the original action (2.16) (see section 3.3 and appendix E). It will be nice to understand this observation at a deeper level.

We move on to compare these results with the gravitational picture. In [4], a family of complex supersymmetric asymptotically AdS_5 solutions of the dual supergravity theory was studied, using earlier results of [44, 45] on general non-supersymmetric black hole solutions. Upon imposing reality conditions on the solutions within this family, one reaches the extremal supersymmetric black hole. The BPS angular velocities of the general complex solutions was defined in [4], using a certain limiting process to the supersymmetric locus, (in the present context of equal angular potentials) as

$$\omega = 2\pi\mathrm{i}\,\tau = 2\pi\mathrm{i}\,\frac{(a-1)(-(a+2)n_0 - 3\mathrm{i}r_+)}{(a+2)^2 + 9\,r_+^2}\,, \tag{4.29}$$

where $a \in [0,1)$ and $r_+ > 0$. At extremality, i.e. for $r_+ = \sqrt{2a+a^2}$, τ reduces to [4]

$$\tau^*(a) = \frac{(a-1)\big(-(a+2)n_0 - 3\mathrm{i}\sqrt{a(a+2)}\big)}{2(a+2)(5a+1)}\,. \tag{4.30}$$

The two values $n_0 = \pm 1$ in (4.29) are related in field theory by $\tau_1 \to -\tau_1$, and label two complex conjugated solutions in the gravitational theory related by $\mathrm{Im}\,\omega \to -\mathrm{Im}\,\omega$. At extremality the metric and gauge field configurations of two gravitational solutions are real, and they coincide which means that the two values $n_0 = \pm 1$ are simply two descriptions of the very same solution. One can check that for $n_0 = \pm 1$ the gravitational extremal curve $\tau^*(a)$ in (4.30) agrees with the field theory extremal curve τ^*, obtained from (4.27) as one expects.[16] We plot these curves in figure 3. The dashed curve in this figure is the same as the $(1,0)$ curve in [8].

[16] We have checked that there are no (m,n) saddles in the $n_0 = -1$ field theory index that matches the $n_0 = +1$ extremal curve. Indeed, once the holographic dictionary is established, it would have been surprising to have two different field-theory saddles corresponding to the same BPS black hole solution.

JHEP09(2020)184

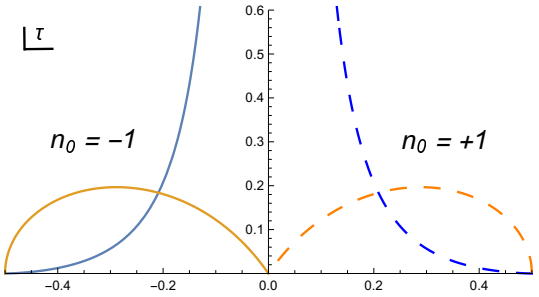

Figure 3. The orange curves are plots of extremal curves τ^*. The blue curves are plots of their entropy as a function of the worldline parameter τ_1. These curves agree with the respective gravitational curves with the same labels. In the gravitational theory the extremal curves for $n_0 = -1$ (solid) and for $n_0 = +1$ (dashed) have the same metric and gauge field configurations.

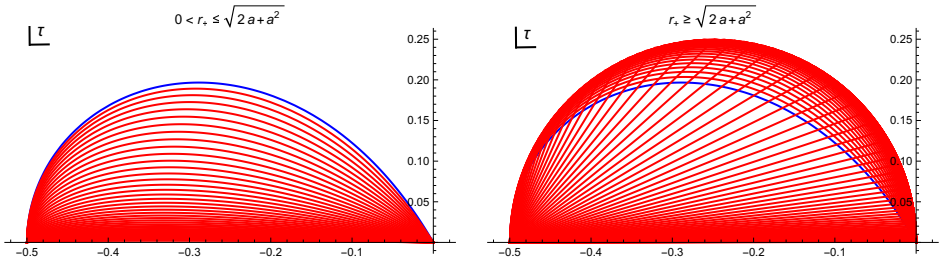

Figure 4. The blue curve denotes the extremal black hole-locus with the horizon radius $r_+ = \sqrt{2a + a^2}$. The red curves correspond to different values of r_+ (where the solution is complex). Notice that the envelope of these complex solutions in $\mathbb{H}$ is bounded by the semi-circle on the right.

In figure 4 we have plotted the regions covered by such solutions as one varies the parameters a and r_+. We note that the known non-extremal supersymmetric solutions discussed in [4] (which have $0 \leq a < 1$ and $r_+ > 0$) do not cover the full range of complex coupling $\tau \in \mathbb{H}$, and, in particular, the regions with large τ_2. As we will see in the following subsections, there are other saddles (m, n) which exist (and dominate) other regions.

4.3 Entropy of (m, n) solutions

In this subsection we extremize the entropy functional of the ensemble described by (m, n) saddles, and calculate their entropy. The procedure is exactly as in the $(1, 0)$ case, namely that the extremization combined with the imposition of reality of the expectation values of field-theory charges and entropy forces the chemical potential τ to live on a specific one-dimensional curve in the upper half plane.

We start by rewritting (4.13) in terms of the variable $\widetilde{\tau} = m\tau + n$,

$$S_{\text{eff}}(m, n; \widetilde{\tau}) = \frac{1}{m} \frac{\pi \mathrm{i}}{27} N^2 \frac{\left(2\widetilde{\tau} + \chi_1(m+n)\right)^3}{\widetilde{\tau}^2} + N^2 \pi \mathrm{i}\, \varphi(m, n)\,. \tag{4.31}$$

We suppress $\varphi(m, n)$ in the following discussion, keeping in mind that it can be reinstated following the discussion in the previous section. To ease presentation we also suppress the

JHEP09(2020)184

dependence of χ on m and n. The entropy of (m,n) saddles is obtained by the following extremization,

$$\mathcal{S}_{(m,n)} = \operatorname*{ext}_{\tau} \mathcal{E}(\tau, J, Q)\,, \tag{4.32}$$

where the entropy functional $\mathcal{E}$ is

$$\mathcal{E}(\tau, J, Q) = -S_{\text{eff}}(m, n; \tau) - 2\pi\mathrm{i}\,\tau\big(2J + Q\big) - \pi\mathrm{i}\,Q\,. \tag{4.33}$$

From the chain rule it follows that

$$\operatorname*{ext}_{\tau} \mathcal{E}(\tau, J, Q) = \operatorname*{ext}_{\widetilde{\tau}} \mathcal{E}(\widetilde{\tau}; \widetilde{J}, \widetilde{Q})\,, \tag{4.34}$$

where we have defined useful auxiliary charges in terms of the physical charges as

$$\widetilde{Q} = Q - 2\,\frac{n}{m}\,(2J + Q)\,, \qquad 2\widetilde{J} + \widetilde{Q} = \frac{2J + Q}{m}\,. \tag{4.35}$$

It should be clear from the above considerations that the entropy of extremal (m,n) solutions has a similar form as that of the $(1,0)$ solution (4.23) with Q, J replaced by $\widetilde{Q}$, $\widetilde{J}$, respectively. We now spell out some of the details.

We have that $\mathcal{S}_{(m,n)}$ is a root of the cubic polynomial $\widetilde{P}(\frac{x}{2\pi\mathrm{i}})$, where

$$\widetilde{P}(x) = \left(-\frac{\chi_1 \widetilde{Q}}{2} + x\right)^3 - \frac{\chi_1\, N^2}{2m}\big(\chi_1 \widetilde{J} + x\big)^2\,, \tag{4.36}$$

$$= \widetilde{p}_0 + \widetilde{p}_1\, x + \widetilde{p}_2\, x^2 + x^3\,, \tag{4.37}$$

with

$$\widetilde{p}_0 = -\chi_1 N^2\,\frac{\widetilde{J}^2}{2m} - \chi_1\,\frac{\widetilde{Q}^3}{8}\,, \qquad \widetilde{p}_1 = \frac{3}{4}\widetilde{Q}^2 - \frac{N^2 \widetilde{J}}{m}\,, \qquad \widetilde{p}_2 = -\frac{3}{2}\,\chi_1\,\widetilde{Q} - \chi_1\,\frac{N^2}{2m}\,. \tag{4.38}$$

Next we impose reality conditions. Notice that reality of (J,Q) is equivalent to reality of $(\widetilde{J},\widetilde{Q})$. Imposing the reality conditions on the charges as well as the entropy $\mathcal{S}_{(m,n)}$, we obtain

$$\widetilde{J}^*(\widetilde{\tau}_1) = \frac{N^2\,(2\widetilde{\tau}_1 + \chi_1)^2(7\widetilde{\tau}_1 - \chi_1)}{432\,m\,\widetilde{\tau}_1^3}\,, \quad \widetilde{Q}^*(\widetilde{\tau}_1) = -\,\frac{N^2\,(2\widetilde{\tau}_1 + \chi_1)(10\widetilde{\tau}_1 - \chi_1)}{72\,m\,\widetilde{\tau}_1^2}\,, \tag{4.39}$$

and the extremal locus

$$\widetilde{\tau}_2^* = \sqrt{\frac{3\widetilde{\tau}_1^2\,(2\,\widetilde{\tau}_1 + \chi_1)}{\chi_1 - 6\widetilde{\tau}_1}}\,. \tag{4.40}$$

Notice that $\widetilde{\tau}_1 = 0$ is a cusp of the curve. The corresponding singularity is related to the phenomenon of the solution at this point becoming infinitely large, which can be seen from the fact that the charges (4.39) become infinite. Excluding this point, and demanding that the expression under the square root in (4.40) is positive gives us the following allowed values of $\widetilde{\tau}_1$:

$$\left.\begin{array}{r} -\frac{1}{2} < \widetilde{\tau}_1 < 0 \\ 0 < \widetilde{\tau}_1 < \frac{1}{6} \end{array}\right\} \qquad \text{if} \quad (m+n) \bmod 3 = 1\,, \tag{4.41}$$

$$\left.\begin{array}{r} 0 < \widetilde{\tau}_1 < \frac{1}{2} \\ -\frac{1}{6} < \widetilde{\tau}_1 < 0 \end{array}\right\} \qquad \text{if} \quad (m+n) \bmod 3 = 2\,. \tag{4.42}$$

JHEP09(2020)184

Note that the real part of the action S_{eff} is less than (greater than) the limiting value of all saddles as $\tau_2 \to \infty$ (which we will discuss in the next section) for the first lines (second lines) in (4.41), (4.42). Relatedly, the first lines reproduce the action and entropy of the known black hole solutions, while the second lines do not correspond to anything that we know of in gravity.[17] For this reason we define the Cardy-like limit (discussed later in more detail) as $\widetilde{\tau} \to 0$, $-\chi_1 \widetilde{\tau}_1 > 0$.

In terms of the physical chemical potential τ, (4.40) takes the forms

$$\tau_2^* = \frac{1}{m}\sqrt{\frac{3\,(m\,\tau_1+n)^2\,(2\,m\,\tau_1+2\,n+\chi_1)}{\chi_1-6\,m\,\tau_1-6\,n}}\,, \tag{4.43}$$

and the first lines of (4.41), (4.42) take the form,

$$\begin{cases} -\frac{1+2\,n}{2m} < \tau_1 < -\frac{n}{m} & \text{if} \quad (m+n)\bmod 3 \;=\; 1\,, \\ -\frac{n}{m} < \tau_1 < \frac{1-2n}{2\,m} & \text{if} \quad (m+n)\bmod 3 \;=\; 2\,. \end{cases} \tag{4.44}$$

From equation (4.36) it follows that $\mathcal{S}_{(m,n)} = 0$ for solutions such that $\chi_1(m+n) = 0$. From now on, we focus on solutions such that $\chi_1 = \pm 1$. The reality conditions on charges and entropy imply that for all $m \in \mathbb{N}$ and $n \in \mathbb{Z}$ with $(m+n)\bmod 3 \neq 0$ the following factorisation property holds

$$\widetilde{p}_0 = \widetilde{p}_1 \widetilde{p}_2\,. \tag{4.45}$$

The factorisation (4.45) implies that the algebraic form of the $\mathcal{S}_{(m,n)}$ is

$$\mathcal{S}_{(m,n)} = \pi\sqrt{3\,\widetilde{Q}^2 - \frac{4N^2\widetilde{J}}{m}}\,. \tag{4.46}$$

The constraint (4.45) can be used to eliminate one variable in this expression. An implicit way to do that, is to use (4.39) in the right-hand side of (4.46). In that way one obtains the following parametric expression for the entropy,

$$\begin{aligned} \mathcal{S}_{(m,n)}(\widetilde{\tau}_1) &= \frac{2\pi N^2}{m}\,\frac{\sqrt{1-8\,\widetilde{\tau}_1^2\big(8\,\widetilde{\tau}_1\,\chi_1+6\,\widetilde{\tau}_1^2+3\big)}}{48\sqrt{3}\,\widetilde{\tau}_1^2} \\ &= \frac{2\pi N^2}{m}\,\frac{\sqrt{1-8\,(m\tau_1+n)^2\big(8\,\chi_1(m\tau_1+n)+6(m\tau_1+n)^2+3\big)}}{48\,\sqrt{3}\,(m\tau_1+n)^2}\,, \end{aligned} \tag{4.47}$$

where the real parameter τ_1 ranges in the domain (4.44).[18]

From equations (4.39) and (4.47) it follows that when the extremal (m,n) curve (4.43) approaches the rational number $-\frac{n}{m}$ within the range (4.44), the expectation value of charges as well as the entropy (in units of N^2) grow to infinity. We refer to such limits as extremal Cardy-like limits (see figure 5). As the set of rationals $\mathbb{Q}$ is dense, it follows that $\tau_2 = 0$ is an accumulation line for such limits. Figure 6 shows a set of extremal curves

[17] From now on we only refer to the regions in the first lines when we discuss extremal curves.

[18] The expression (4.47) is independent of the phase φ even if we reinstate it in the preceding discussion.

JHEP09(2020)184

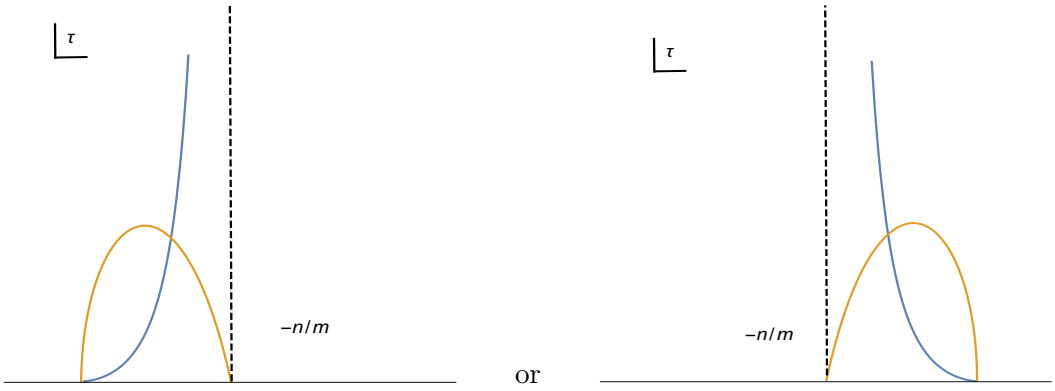

Figure 5. The orange lines are extremal curves in the τ-plane for the (m,n) saddle (where J, Q, and $\mathcal{S}_{(m,n)}$ are all real). The blue line plots the normalized entropy $\frac{\mathcal{S}_{(m,n)}}{N^2}$ along the corresponding extremal curve. For every $\frac{n}{m}$, with $m > 0$, $\gcd(m,n) = 1$, and such that $(m+n) \bmod 3 \neq 0$, the normalized entropy grows to $+\infty$ when the extremal curve approaches $-\frac{n}{m}$ from the left ($(m+n) \bmod 3 = 1$), or from the right ($(m+n) \bmod 3 = -1$).

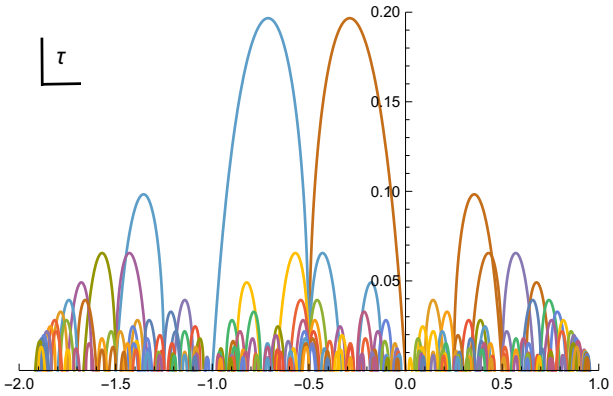

Figure 6. The extremal curves in the fundamental domain $-2 \leq \tau_1 < 1$, from $m = 1, \ldots, 30$ and $n = -30, \ldots, 30$.

for $m = 1, \ldots, 30$ and $n = -30, \ldots, 30$. In the J-Q plane, the extremal solution for $(1,0)$ is the one-dimensional curve (4.21) or, equivalently, (4.28). Now we see that there is a dense set of such extremal curves (4.45) in the J-Q plane labelled by rational numbers.

It would be very interesting to find the gravitational interpretation of the generic (m,n) saddles. These should be asymptotically AdS_5 supersymmetric solutions whose Bekenstein-Hawking entropy should coincide with our predictions (4.46), (4.47).[19] An interesting feature of the (m,n) saddles is that the labels of the set of saddle-points i.e. (m,n) with $\gcd(m,n) = 1$, can be equivalently thought of as the coset $\Gamma_\infty \backslash \Gamma$, i.e. the set of matrices in $\Gamma = \mathrm{SL}(2,\mathbb{Z})$ (acting as usual via fractional linear transformations on τ) modulo the subgroup Γ_∞ that fixes the point at infinity. This is the same structure as the AdS_3 black hole Farey Tail [49], and perhaps points to a similar structure of Euclidean saddle-points as in [50].

[19] The hairy black holes explored in [46–48] could be relevant to this discussion.

JHEP09(2020)184

4.4 Phase structure

Now we analyze the relative dominance of the saddles for a given value of τ. Firstly, recall that $\mathcal{I}(\tau)$ is invariant under $\tau \to \tau + 3$, and correspondingly we analyze the region $-2 \leq \mathrm{Re}(\tau) < 1$. The idea is to compare the real parts of the action at the different saddles at a generic point in the τ-plane. The dominant phase (if a unique one exists) is the saddle with least real action. The phase boundaries where the real parts of the actions of two saddles are equal are called the anti-Stokes lines.

As $\tau_2 \to \infty$, the real part of the action (4.12) of all the phases with $(m+n) \bmod 3 = 0$ equals $-\frac{8}{27}\pi N^2 \tau_2$. There are an infinite number of such phases and the imaginary parts and sub-dominant effects will be important to evaluate the path integral. (Curiously, the entropy of these saddles actually vanish as shown in the previous subsection.) When $(m+n) \bmod 3 \neq 0$, then the third term in (4.12) is always positive, and it dominates over the second term for large enough τ_2. Therefore these saddles are sub-dominant compared to those with $(m+n) \bmod 3 = 0$ in that region. When we start to reduce τ_2 we begin to hit regions where one phase dominates. For example, the action $S_{\text{eff}}(1,0;\tau)$ blows up at $\tau = 0$ and the dominant phase near $\tau = 0$ is $(1,0)$ (the black hole). The anti-Stokes lines between the black hole and the region at $\tau_2 \to \infty$ is given by

$$\mathrm{Re}\, S_{\text{eff}}(1,0;\tau) = -\frac{8}{27}\pi N^2 \tau_2 \implies \left(\tau_1 + \frac{1}{6}\right)^2 + \tau_2^2 = \frac{1}{36}\,. \tag{4.48}$$

Similarly, as τ approaches a rational point $-\frac{n}{m}$, $-\mathrm{Re}\, S_{\text{eff}}(m,n;\tau)$ becomes very large and that is the corresponding dominant phase near the point.

In figures 7, 8, we have plotted the phase diagram for $\{(m,n) \mid m = 0, \ldots 10, n = -10, \ldots, 10\}$. Figure 7 is plotted for $\tau_2 > 0.1$ where we only see the dominance of $(1,0)$ (which dominates below the semi-circle (4.48))[20] and $(1,1)$ (which dominates below a semi-circle isomorphic to (4.48) but translated to the left by $\frac{2}{3}$) apart from the ones that dominate as $\tau_2 \to \infty$ (i.e. $(m+n) \bmod 3 = 0$).[21]

4.5 Cardy-like limit(s) revisited

In this subsection we revisit the Cardy-like limit at finite N of the SU(N) $\mathcal{N} = 4$ SYM superconformal index (2.9), with $n_0 = -1$. As mentioned in the introduction, this limit has been analyzed for a class of $\mathcal{N} = 1$ SCFTs including $\mathcal{N} = 4$ SYM. Here the scope is to address the problem from a different angle, by using the results presented so far.

First of all, it is clear from the formula (4.12) that the dominant contribution to the large-N expansion of the index (4.1) in the Cardy-like limit, $\tau \to 0$ with $\tau_1 < 0$,[22] comes from the $(1,0)$ saddle which we identified with the black hole in the previous section. The

[20] This region lies inside the region in red in the figure 4 to the right which means that there is a supersymmetric (but not necessarily extremal) black-hole-like solution that exists in supergravity).

[21] A partial phase diagram for $\mathcal{N} = 4$ SYM was first presented in [8]. It focused on the subset of $(1,r)$ configurations, with $r \in \mathbb{Z}$ which is equivalent to our figure 7 after mapping conventions (see Footnote 32).

[22] The second condition is important because the sign of the second term in (4.12), which dominates in absolute value as $\tau \to 0$, is controlled by $\mathrm{sgn}(\tau_1)$.

JHEP09(2020)184

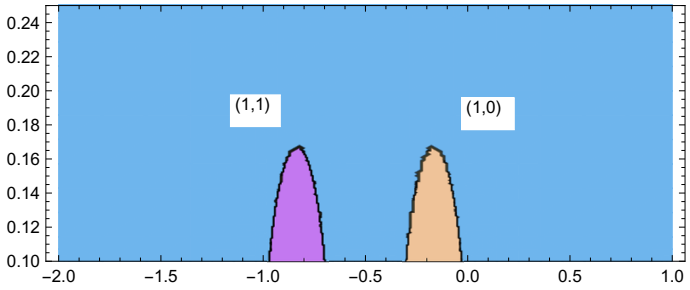

Figure 7. The phase structure for $\tau_2 \geq 0.1$. Apart from the phases $\tau_2 \to \infty$, there are two dominant phases $(1,0)$ and $(1,1)$ in the semi-circular regions. Here we have scanned $\{(m,n) \mid m = 0,\dots 30, n = -30,\ \dots, 30\}$ with $\gcd(m,n) = 1$.

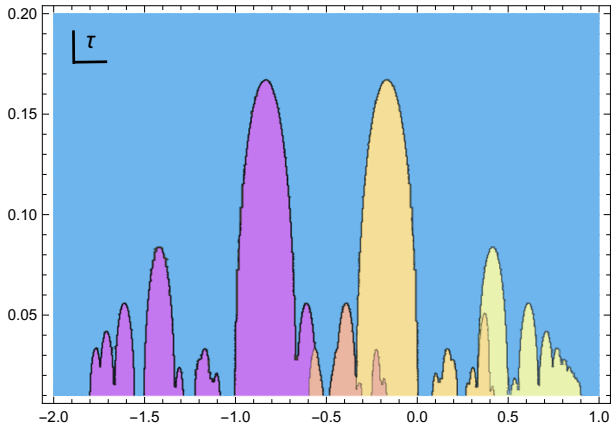

Figure 8. The phase structure for $\tau_2 \geq 0.01$. Here we see that new phases appear close to the real axis, near rational points. Here we have scanned $\{(m,n) \mid m = 0,\dots 10, n = -10,\ \dots, 10\}$ with $\gcd(m,n) = 1$.

large-N action of $(1,0)$ saddle in this limit is

$$S_{\text{eff}}(1,0;\tau) \underset{\tau\to 0}{\longrightarrow} \frac{\pi \mathrm{i} N^2}{27}\left(\frac{1}{\tau^2}+\frac{6}{\tau}\right). \tag{4.49}$$

In fact one can do better and go beyond the large-N limit in the Cardy-like limit. We start with the formulas (3.6), (3.17), (3.20) and take the $\tau \to 0$ limit. We obtain

$$\begin{aligned} \log Q(z;\tau) &\underset{\tau\to 0}{\longrightarrow} \frac{1}{4\pi^2\tau^2}\sum_{\substack{m\in\mathbb{Z}\\ m\neq 0}} \frac{\mathbf{e}(-mz_1)}{m^3}, \\ &= \frac{\pi \mathrm{i}}{3}\frac{1}{\tau^2} B_3\big(\{z_1\}\big). \end{aligned} \tag{4.50}$$

Similarly, for the P function we obtain, from (3.6),

$$\log|P(z;\tau)| \underset{\tau\to 0}{\longrightarrow} -\frac{\pi\tau_2}{|\tau|^2} B_2\big(\{z_1\}\big), \tag{4.51}$$

with holomorphic part

$$\log P(z;\tau) \underset{\tau\to 0}{\longrightarrow} -\frac{\pi \mathrm{i}}{\tau} B_2\big(\{z_1\}\big). \tag{4.52}$$

JHEP09(2020)184

From (3.26) we have

$$S(u) \underset{\tau\to 0}{\longrightarrow} \pi \mathrm{i} \sum_{i,j} \left(\frac{1}{3\tau^2} \left(B_3\left(\{u_{1ij}\}\right) + 3B_3\left(\{u_{1ij}+\tfrac{1}{3}\}\right)\right) + \frac{1}{\tau}\left(B_2\left(\{u_{1ij}\}\right) - B_2\left(\{u_{1ij}+\tfrac{1}{3}\}\right)\right)\right). \tag{4.53}$$

The formula (4.53) is precisely the one obtained in the Cardy-like limit studied in [14]. We note, however, that our starting point here is different and that we do not need to go through the subtleties of the Cardy-like limit that were used in [14]. The action (4.53) can be then used for the finite N answer in the Cardy-like limit as in [14], to obtain (4.49). The advantage of our formalism is that we can calculate further corrections in that limit in a systematic way, using the Fourier expansions (in τ_1) of the Eisenstein series [26].

The considerations in section 2 allows to clarify one more aspect of the Cardy-like limit. In [14] we analyzed the different saddles of the theory in the large-N limit along the real line. Now we can repeat that analysis for finite N. The right-hand side of (4.53) only depends on u_1, it is differentiable, and periodic with period 1, and thus obeys the conditions of the Lemma in subsection 2.1. For N finite and prime, its Cardy-like saddles are $(0,0)$ and $(0,1)$. Their actions (after properly dealing with the $i=j$ modes in (4.53)) are,[23] (as $\tau\to 0$ and exact in N),

$$S_{\text{eff}}^{(0,0)}(\tau) = \frac{\pi \mathrm{i} N^2}{27}\left(\frac{1}{\tau^2}+\frac{6}{\tau}\right) - \frac{\pi i N}{6\tau} + O(\tau^0)\,, \tag{4.54}$$

$$S_{\text{eff}}^{(0,1)}(\tau) = \frac{\pi \mathrm{i}}{27}\left(\frac{\chi_1(N)}{N}\frac{1}{\tau^2}+\frac{6}{\tau}\chi_0(N)\right) - \frac{\pi i N}{6\tau} + O(\tau^0)\,. \tag{4.55}$$

These results are consistent with the intuition of a large-N limit followed by Cardy-like limit: in the Cardy-like limit the $(1,0)$ saddle approaches the $(0,0)$ and the other large-N saddles approach the $(0,1)$. Indeed the term proportional to N^2 in (4.54) coincides with (4.49), and that in (4.55) vanishes as does $S_{\text{eff}}(0,1;\tau)$. In appendix D we expand on the role of the $(0,0)$ saddle further. At finite $N>2$, and in the Cardy-like limit $\tau\to 0$ with $\tau_1<0$, the saddle (4.54) dominates, as shown in [14] for a generic family of $\mathcal{N}=1$ SCFTs including $\mathcal{N}=4$ SYM. For the limit $\tau\to 0$ with $\tau_1>0$, the solution (4.55) dominates. A more refined statement about this case involves the use of a higher order expansion in τ with N-dependent coefficients. We postpone such an analysis.

More generally, there exists a Cardy-like limit for all (m,n) saddles (corresponding to a rational $-\frac{n}{m}$ with $(m+n) \bmod 3 \neq 0$), which is $\widetilde{\tau}\to 0$. From Formula (4.10) it follows that the (m,n) saddle is the leading configuration in that limit. As for the $(1,0)$ case mentioned above, the result is sensitive to the actual limiting procedure. As mentioned below equation (4.42) we can define the Cardy-like limit to be $\widetilde{\tau}\to 0$ with $-\chi_1(m+n)\widetilde{\tau}_1>0$. In this limit, the real part of the effective action goes to $-\infty$. For $\chi_1(m+n)=+1(-1)$, the left(right) extremal curve drawn in figure 5 defines a particular example of this limit.

[23] Here we have used the following identity that holds for $z\in\mathbb{R}$ and any integer n with $\gcd(N,|n|)=1$ and $k>1$

$$\sum_{i,j=1}^{N} B_k\left(\left\{z+\frac{n\,(i-j)}{N}\right\}\right) = \frac{1}{N^{k-2}} B_k\left(\{Nz\}\right).$$

JHEP09(2020)184

It is interesting to recast the discussion in the above paragraph in terms of the microcanonical ensemble. Naively, the Cardy-like limit is one in which all the charges scale to infinity and, correspondingly, $\tau \to 0$. However, as we saw above, there is actually a family of interesting limits in which only $\tau_2 \to 0$ and τ_1 approaches a rational number. The microcanonical analog of these new limits has to do with the ambiguity in taking the "large-charge limit" when there are multiple charges. In our situation, equations (2.11), (2.10) imply that τ couples to $2J+Q$, which should scale to infinity. However, the charges J and Q are a priori independent and one needs to specify in what relative manner they scale to infinity. Demanding that the entropy is real specifies a certain relation between the charges. As we discussed in section 4.3, there is a consistent relation for every (m, n) which defines a one-dimensional sector of BPS states in the charge space, such that the corresponding entropy is $\mathcal{S}_{m,n}(J, Q)$. Recalling from [14] that the Cardy limit for $(1, 0)$ is given by $Q \sim \Lambda^2$, $J \sim \Lambda^3$, it is easy to see that the Cardy-like limit for a given (m, n) is given simply by scaling the appropriate linear combinations in the same manner, i.e. $\widetilde{Q} \sim \Lambda^2$, $\widetilde{J} \sim \Lambda^3$.

5 Summary and discussion

In this paper we have found a family of saddle points of the matrix model governing the index of $\mathcal{N} = 4$ SYM on $S^3 \times S^1$. The solution of this problem is governed by the Bloch-Wigner elliptic dilogarithm function which is a well-defined real-analytic function on the torus $\mathbb{C}/(\mathbb{Z}\tau + \mathbb{Z})$ and transforms like a Jacobi form with weight $(0, 1)$ under $\mathrm{SL}(2, \mathbb{Z})$ transformations of the torus. The Bloch formula, which expresses the elliptic dilogarithm as a real-analytic Kronecker-Eisenstein series (a particular type of lattice sum), makes the analysis very elegant. The action at any saddle can be calculated by reading off the zeroth Fourier coefficient of the series along the direction of the saddle. We also develop a second method to calculate the action which uses a series representation of the meromorphic elliptic Gamma functions involved in the original definition of the SYM index. We show that deforming the original action to the Bloch-Wigner type function away from the real axis in this approach agrees with our first approach. Using our formalism we find a family of solutions labelled by (m, n) with $\gcd(m, n) = 1$, and analyze the competition among these phases of the theory at finite τ.

The analysis of this paper relates in a natural way to the various approaches to the problem that have been used so far, and shows that they are all consistent with each other. Firstly, the contact with supergravity comes from the fact that the action of the saddle $(1, 0)$ is precisely the supergravity action of the black hole. We also calculate the action and entropy of the generic (m, n) saddle. It is an interesting question to identify the corresponding gravitational configurations. Secondly, the calculations in the Cardy-like limit get clarified and simplified as the limit $\tau \to 0$ of the finite-τ answer. The formalism is powerful and can be used to calculate corrections from the Cardy-like limits. Thirdly, there seems to be a relation to the Bethe-ansatz type analysis which is intrinsically a meromorphic analysis. We find that the action of the original mermomorphic elliptic gamma function at the Bethe roots agrees with the action at the saddle-points derived from our approach.

JHEP09(2020)184

This makes it clear that the Bethe roots should indeed be identified with Euclidean saddle points of the matrix model.

The relation between the meromorphic approach and our real-analytic approach remains experimental and it would be nice to understand it at a deeper level. In particular, the global analysis of the contour deformations and of the contributions of the saddle-points at different points in moduli space remains to be done. Towards this end it may be important to understand the meromorphic function $\log Q$ (as opposed to just the real part $\log|Q|$) better. It seems to us that this should be related to a multi-valued function studied in [39, 40]. The meromorphic function in question discussed in [39, 40] satisfies a certain first-order differential equation in τ (it is the primitive of a holomorphic Kronecker-Eisenstein series), and trying to find such an equation may be one way to completely fix the phase ambiguities that we discussed in this paper. It is interesting to note that there is also a version of the dilogarithm [51–53] which seems to be closer to the original elliptic gamma function.

The elliptic dilogarithm (in its real-analytic as well as its meromorphic avatars) has been understood in recent years to play a crucial role in string scattering amplitudes (see e.g. [54, 55]). It would be remarkable if there is a direct physical relation between these two appearances. One natural speculation along these lines would be about a *holographic* relation, with the string amplitudes (perhaps suitably modified) being observables in a bulk theory dual to the SYM theory that we discuss in this paper. A less striking, but nevertheless interesting, possibility would be the following syllogism: the appearance of the same elliptic dilogarithm in string scattering amplitudes and the partition function of AdS_5 black holes could be compared with the appearance of the theta function in string amplitudes and the partition functions of black holes in flat space.

Our analysis also clarifies the role of modular symmetry in this problem. The SYM index itself is not a modular form, instead the Bloch-Wigner function is essentially a period function for the real part of the action of the SYM. More precisely, writing the action as a simple linear combination of the functions $\log P$ and $\log Q$ (see equation (3.26)), we have that $\log|P|$ is Jacobi invariant while the Bloch-Wigner dilogarithm is a period function of $\log|Q|$ (see equation (3.16)). In particular, this explains the fact that the SYM action on $S^1 \times S^3$ as $\tau \to 0$ has a τ^{-2} behavior in contrast with the τ^{-1} behavior of holomorphic modular forms appearing in theories on $S^1 \times S^1$.

There are clearly many interesting things to do. For one, our analysis can be enlarged to include 4d $\mathcal{N} = 1$ SCFTs. In another direction, these ideas could lead to progress in similar problems in other dimensions. It would be nice to find the correct mathematical structures to extend the ideas in this paper away from the restriction $\tau = \sigma$. At a technical level, it would be nice to find a direct physical interpretation of the elliptic deformation in the complex plane of the SYM index, the obvious thing to look for would be a supersymmetry-exact operator. Similarly, it would be nice to find a direct relation to the Bethe-ansatz approach, for which there are clues mentioned in this paper.

Finally, it is tempting to speculate that deeper number-theoretical aspects of the functions appearing here play a role in physics. The original motivations of Bloch in uncovering his beautiful formulas arose from algebraic K-theory. Relatedly, the values of the elliptic

JHEP09(2020)184

dilogarithm at particular (algebraic) values of τ are closely related to values of certain L-functions of Hecke characters, and the so-called Mahler measure [56]. It would be really interesting if the physics of SYM and AdS_5 black holes is directly related to these objects, perhaps in a manner that extends the beautiful ideas described in [57].

Acknowledgments

It is a pleasure to thank Dionysios Anninos, Francesco Benini, Francis Brown, Davide Cassani, Atish Dabholkar, Yan Fyodorov, Stavros Garoufalidis, Mahir Hadzic, Dario Martelli, Oliver Schlotterer, Don Zagier for useful and interesting discussions. This work was supported by the ERC Consolidator Grant N. 681908, "Quantum black holes: A macroscopic window into the microstructure of gravity", and by the STFC grant ST/P000258/1.

A Some special functions and their properties

Bernoulli polynomials. The Bernoulli polynomials $B_k(z)$ are defined through the following generating function,

$$\frac{t\,\mathrm{e}^{z\,t}}{(\mathrm{e}^t-1)}=\sum_{k=0}^{\infty}B_k(z)\,\frac{t^k}{k!}\,. \tag{A.1}$$

The first three Bernoulli polynomials are

$$B_1(z)=z-\frac{1}{2}\,, \tag{A.2}$$

$$B_2(z)=z^2-z+\frac{1}{6}\,, \tag{A.3}$$

$$B_3(z)=z^3-\frac{3\,z^2}{2}+\frac{z}{2}\,. \tag{A.4}$$

These polynomials obey the following properties for $z\in\mathbb{C}$,

$$B_k(z)=(-1)^k B_k(z-1)\,, \tag{A.5}$$

$$B_k(z+1)-B_k(z)=\,k\,z^{k-1}\,. \tag{A.6}$$

Their Fourier series decomposition, for $k\geq 2$ and $0\leq x<1$ is

$$B_k(x)=-\frac{k!}{(2\pi\mathrm{i})^k}\sum_{j\neq 0}\frac{\mathbf{e}(jx)}{j^k}\,. \tag{A.7}$$

Clearly this also equals $B_k(\{x\})$ where $\{x\}\coloneqq x-\lfloor x\rfloor$ is the fractional part of z. In particular we have for $x\in\mathbb{R}$

$$B_2(\{x\})=\frac{1}{2\pi^2}\sum_{j\neq 0}\frac{\mathbf{e}(jx)}{j^2}\,, \tag{A.8}$$

$$B_3(\{x\})=-\frac{3\,\mathrm{i}}{4\pi^3}\sum_{j\neq 0}\frac{\mathbf{e}(jx)}{j^3}\,. \tag{A.9}$$

JHEP09(2020)184

Multiple Bernoulli Polynomials. The multiple Bernoulli Polynomials $B_{r,n}(z|\underline{\omega})$ are defined for $z \in \mathbb{C}$, $\underline{\omega} = (\omega_{r-1}, \ldots, \omega_0)$ with $\omega_j \in \mathbb{C} - \{0\}$ through the following generating function [58, 59] (we follow the conventions of [59]):

$$\frac{t^r e^{z\,t}}{\prod_{j=0}^{r-1}(e^{\omega_j\,t}-1)} = \sum_{k=0}^{\infty} B_{r,k}(z|\,\underline{\omega})\,\frac{t^k}{k!}\,. \tag{A.10}$$

The first three cases are

$$B_{1,1}(z|\,\omega_0) = \frac{z}{\omega_1} - \frac{1}{2}\,, \tag{A.11}$$

$$B_{2,2}(z|\,\omega_1,\,\omega_0) = \frac{z^2}{\omega_0\,\omega_1} - \frac{(\omega_0+\omega_1)\,z}{\omega_0\,\omega_1} + \frac{\omega_0^2+3\,\omega_0\,\omega_1+\omega_1^2}{6\,\omega_0\,\omega_1}\,, \tag{A.12}$$

$$\begin{aligned} B_{3,3}(z|\,\omega_2,\,\omega_1,\,\omega_0) = {} & \frac{\left(z+\frac{1}{2}(-\omega_0-\omega_1-\omega_2)\right)^3}{\omega_0\,\omega_1\,\omega_2} \\ & - \frac{\left({\omega_0}^2+{\omega_1}^2+{\omega_2}^2\right)\left(z+\frac{1}{2}(-\omega_0-\omega_1-\omega_2)\right)}{4\,\omega_0\,\omega_1\,\omega_2}\,. \end{aligned} \tag{A.13}$$

The multiple Bernoulli polynomials are symmetric under permutations of components in $\underline{\omega}$. They obey the following periodicity property

$$B_{k,k}(z\,|\,\underline{\omega}[j]) = -B_{k,k}(z+\omega_j\,|\,\underline{\omega})\,, \tag{A.14}$$

where $\omega[j] \coloneqq (\omega_{k-1}, \ldots, -\omega_j, \ldots, \omega_0)$. Moreover, they can be expanded in terms of usual Bernoulli polynomials. In particular, we have

$$B_{1,1}(z-1\,|\,-1) = -\,B_1(z)\,, \tag{A.15}$$

$$B_{2,2}(z-1\,|\,\omega_1,-1) = -\frac{1}{\omega_1}\,B_2(z) + B_1(z) - \frac{\omega_1}{6}\,, \tag{A.16}$$

$$\begin{aligned} B_{3,3}(z-1\,|\,\omega_2,\,\omega_1,-1) = {} & -\frac{1}{\omega_1\,\omega_2}\,B_3(z) + \frac{3\,(\omega_1+\omega_2)}{2\,\omega_1\,\omega_2}\,B_2(z) \\ & - \frac{1}{2}\left(\frac{\omega_1}{\omega_2}+\frac{\omega_2}{\omega_1}+3\right)B_1(z) + \frac{\omega_1+\omega_2}{4}\,. \end{aligned} \tag{A.17}$$

One has similar formulas which express $B_{n,n}(z|\,\underline{\omega})$ with $\omega_0 = 1$ in terms of usual Bernoulli polynomials, to obtain those, one uses (A.15), (A.16), (A.17) and applies the property (A.14) on the corresponding left-hand sides. The above equation will be convenient to analytically-match the results of the action in appendix E and section 4.

Theta functions. The odd Jacobi theta function is defined as (with $q = \mathbf{e}(\tau)$, $\zeta = \mathbf{e}(z)$)

$$\vartheta_1(z) = \vartheta_1(z;\tau) \coloneqq -\mathrm{i}\sum_{j\in\mathbb{Z}} (-1)^j\, q^{\frac{1}{2}(j+\frac{1}{2})^2}\zeta^{(j+\frac{1}{2})}\,. \tag{A.18}$$

In the main text we use the following function

$$\theta_0(z;\tau) \coloneqq -\zeta^{\frac{1}{2}}\,q^{\frac{1}{24}}\,\frac{\vartheta_1(z,\tau)}{\eta(\tau)} = (1-\zeta)\prod_{j=1}^{\infty}(1-q^j\zeta)\,(1-q^j\zeta^{-1})\,. \tag{A.19}$$

JHEP09(2020)184

The function $\theta(z)$ is holomorphic and has simple zeros at $z = j\tau+\ell$, $j,\ell \in \mathbb{Z}$. The following elliptic transformation properties follows easily from the definition,

$$\theta_0(z+1;\,\tau) = \theta_0(z;\,\tau)\,, \tag{A.20}$$

$$\theta_0(z+\tau;\,\tau) = -\mathbf{e}(-z)\,\theta_0(z) = \theta_0(-z;\,\tau)\,. \tag{A.21}$$

Modular properties of $\boldsymbol{\theta_0}$ and $\boldsymbol{\Gamma_e}$. In the main text we also introduced the elliptic gamma function in (2.15) which obeys the quasi-periodicity property (3.10). The function $\Gamma_e(z,\tau,\sigma)$ is meromorphic, it has simple zeros at $z = (j+1)\tau+(k+1)\sigma+\ell$ and simple poles at $z = -j\tau - k\sigma + \ell$, $j,k \in \mathbb{N}_0$, $\ell \in \mathbb{Z}$. Next, we introduce a set of identities that involve modular transformations of parameters τ, σ and z. Recall that both θ_0 and Γ_e are invariant under the transformation $z \mapsto z - k_0$ for $k_0 \in \mathbb{Z}$. We will combine this symmetry with the modular transformation properties to obtain new identities. For θ_0 we have, for every $k_0 \in \mathbb{Z}$,

$$\theta_0(z;\tau) = \exp\big(\pi \mathrm{i} B_{2,2}(z-k_0|\tau,-1)\big)\,\theta_0\left(\frac{z-k_0}{\tau};-\frac{1}{\tau}\right). \tag{A.22}$$

Using (A.20), (A.21), we can also write this as

$$\theta_0(z;\tau) = \exp\big(-\pi \mathrm{i} B_{2,2}(z-k_0|\tau,1)\big)\,\theta_0\left(-\frac{z-k_0}{\tau};-\frac{1}{\tau}\right). \tag{A.23}$$

The analogous identities for elliptic Gamma functions are, for $\mathrm{Im}(\frac{\sigma}{\tau}) > 0$, $k_0 \in \mathbb{Z}$, which are minor variations of the ones presented in [35, 59],

$$\Gamma_e(z;\tau,\sigma) = \exp\left(\frac{\pi i}{3} B_{3,3}(z-k_0|\tau,\,\sigma,-1)\right) \frac{\Gamma\left(\frac{z-k_0}{\tau};-\frac{1}{\tau},\frac{\sigma}{\tau}\right)}{\Gamma\left(\frac{z-k_0-\tau}{\sigma};-\frac{1}{\sigma},-\frac{\tau}{\sigma}\right)}\,, \tag{A.24}$$

$$\Gamma_e(z;\tau,\sigma) = \exp\left(-\frac{\pi i}{3} B_{3,3}(z-k_0|\tau,\sigma,1)\right) \frac{\Gamma\left(-\frac{z-k_0}{\sigma};-\frac{1}{\sigma},-\frac{\tau}{\sigma}\right)}{\Gamma\left(-\frac{z-k_0-\sigma}{\tau};-\frac{1}{\tau},\frac{\sigma}{\tau}\right)}\,. \tag{A.25}$$

Factorization properties. For our purposes it will be important to use the following "factorization" identity of θ_0. For all $m \in \mathbb{N}$ we have[24]

$$\theta_0(z;\,\tau) = \prod_{\ell_1=0}^{m-1} \theta_0(z+\ell_1\tau;\,m\tau)\,. \tag{A.26}$$

Upon using this factorization identity, the symmetry of θ_0 under integer shifts of its second argument, and the modular identity (A.22), one obtains, for any $k_0(\ell) \in \mathbb{Z}$, $\ell = 0,\ldots,m-1$,

$$\theta_0(z;\,\tau) = \prod_{\ell=0}^{m-1} \exp\big(\pi \mathrm{i}\, B_{2,2}(z-k_0(\ell)+\ell\tau|m\tau+n,-1)\big)\,\theta_0\left(\frac{z-k_0(\ell)+\ell\tau}{m\tau+n};-\frac{1}{m\tau+n}\right). \tag{A.27}$$

[24] This identity can be proven with the use of the representation (C.1) and basic trigonometric identities.

JHEP09(2020)184

We also have similar factorization identities of $\Gamma_{\rm e}$ [35][25]

$$\begin{aligned}\Gamma_{\rm e}(z;\tau,\tau) &= \prod_{\ell_1,\ell_2=0}^{m-1} \Gamma_{\rm e}(z+(\ell_1+\ell_2)\tau\,;\, m\,\tau,\, m\,\tau)\,,\\ &= \prod_{\ell=0}^{2(m-1)} \Gamma_{\rm e}(z+\ell\tau\,;\, m\,\tau,\, m\,\tau)^{m-|\ell-m+1|}\,.\end{aligned} \tag{A.28}$$

Upon using this factorization identity, the symmetry of $\Gamma_{\rm e}$ under integer shifts of its last two arguments, and the appropriate limit of modular identity (A.24), one obtains, with $\tau^\varepsilon = \tau+\varepsilon$, $\varepsilon\to 0$, and for any $k_0(\ell)\in\mathbb{Z}$, $\ell=1,\ldots,m$,

$$\begin{aligned}\Gamma_{\rm e}(z;\,\tau,\,\tau) = \prod_{\ell=0}^{2(m-1)} &\exp\left(\frac{\pi \mathrm{i}}{3}\, B_{3,3}(z-k_0(\ell)+\ell\tau|m\tau+n, m\tau+n, -1)\right)\\ &\times \frac{\Gamma_e\left(\frac{z-k_0+\ell\tau}{m\tau+n}; -\frac{1}{m\tau+n}, \frac{m\tau^\varepsilon+n}{m\tau+n}\right)}{\Gamma_e\left(\frac{z-k_0+\ell\tau-(m\tau+n)}{m\tau^\varepsilon+n}; -\frac{1}{m\tau^\varepsilon+n}, -\frac{m\tau+n}{m\tau^\varepsilon+n}\right)}\,.\end{aligned} \tag{A.29}$$

B Elliptic extension: zeroes and poles

In this appendix we comment on the singularities of the elliptically extended action that was introduced in section 3.2. The integrand of the SYM index (3.23) can be rewritten in terms of the function $Q_{a,b}$ which was introduced in (3.21) as, for $u\in\mathbb{C}$,

$$\mathcal{Q}(u) \coloneqq \left|Q_{1,0}(u)\,Q_{1,0}(-u)\right|^{-1} \left|Q_{-\frac{1}{3},\frac{1}{3}}(u)\,Q_{-\frac{1}{3},\frac{1}{3}}(-u)\right|^{-3}. \tag{B.1}$$

Here the $Q_{1,0}$ factors arise from the vector multiplet, and the $Q_{-\frac{1}{3},\frac{1}{3}}$ factors arise from the chiral multiplets.

The action has singularities whenever the function $\mathcal{Q}$ has singularities or zeros. In figure 9 we present the positions of zeros (blue) and singularities (red and green) of $\mathcal{Q}$ in the u-plane. The zeros come from the vector multiplet, the singularities come from the chiral multiplets. As $\left|Q_{-\frac{1}{3},\frac{1}{3}}(u)\,Q_{-\frac{1}{3},\frac{1}{3}}(-u)\right|^{-1}$ is elliptic, the full set of zeros and poles are lattice translates of those in the fundamental domain $0\le u_1<1$ and $0\le u_2<1$. In this domain, $|\Gamma_e(u+\frac{2}{3}\tau+\frac{1}{3})\Gamma_e(-u+\frac{2}{3}\tau+\frac{1}{3})|$ has a single pole at $\frac{2\tau+1}{3}$ and it has no zero, and $|P(u-\frac{1}{3}\tau+\frac{1}{3})|^{u_2}$ has a zero of order $\frac{1}{3}$ at $\frac{\tau+2}{3}$ and it has no singularity. Further, in this domain, $|P(-u-\frac{1}{3}\tau+\frac{1}{3})|^{-u_2}$ has a singularity of order $\frac{2}{3}$ at $\frac{2\tau+1}{3}$ and it has no zero. It thus follows that $\left|Q_{-\frac{1}{3},\frac{1}{3}}(u)\,Q_{-\frac{1}{3},\frac{1}{3}}(-u)\right|^{-1}$ has two singularities of order $\frac{1}{3}$, located at the green and red points, respectively, in figure 9. An analogous analysis shows that the only zeroes of (B.1) in the fundamental domain come from the vector multiplet contribution, i.e. from the first factor in right-hand side of (B.1) (the blue points in the figure).

For configurations that pass through the zeroes or singularities of $\mathcal{Q}$, the effective action $S(u)$ is $+\infty$ or $-\infty$, respectively. Indeed, the original contour of integration defining the SYM index crosses the zeroes of $\mathcal{Q}$. In order to deal with this issue, one can turn on a

[25] This identity can be proven with the use of the representation (C.3) and basic trigonometric identities.

JHEP09(2020)184

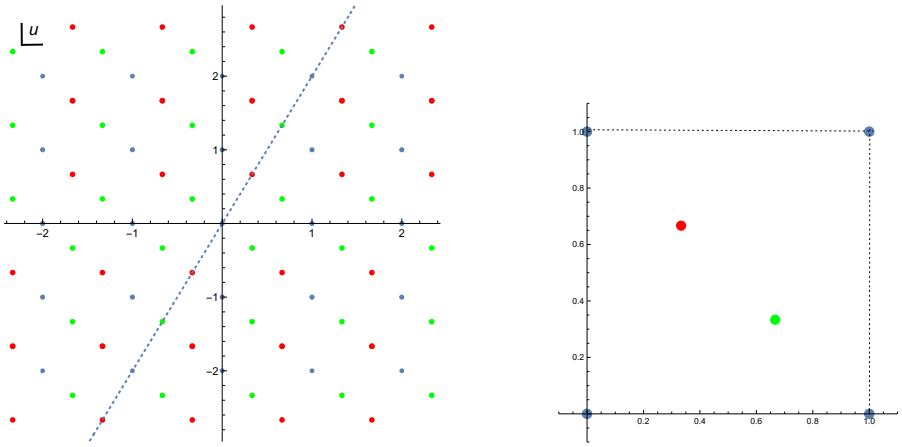

Figure 9. The zeroes and singular points of $\mathcal{Q}$. Blue points are zeroes of the vector multiplet contribution. Red and green points are singularities of the chiral multiplet contributions. The red ones are singularities of the undressed elliptic Gamma functions, while the green ones are singularities that come from the dressing factor $P(z)^{z_2}$ in equation (3.7) (see also (3.21)). Both singularities are of order one and the zeroes are of order two. The horizontal unit stands for 1 and the vertical unit stands for τ.

regulator ϵ, following the prescription introduced in [4], (and which will be recalled in the following section). This regulator shifts the position of zeroes and singularities in the u-plane by an amount proportional to ϵ in a direction parallel to the dashed line, thus making the contour integrals that define the actions of saddles $(0,1)$ and $(1,0)$ well-defined.[26] We note that this regulator does not work if the saddle is along the direction $2\tau+1$ (indicated by the dashed lines in figure 9). For this saddle a different regularization must be used. For instance, one such possibility is to turn on flavour fugacities that shift the position of the zeroes and singularities off the dashed line, and in the end take the fugacities to zero.

C Series representations of $\log\theta_0$ and $\log\Gamma_e$

In the main text we calculated the effective action as integrals of elliptic functions constructed out of $\log\theta_0(u)$ and $\log\Gamma_e(u)$, along various directions in the complex u-plane, using the double Fourier expansion in u provided by the Bloch formula (see the discussion in section 4.1). In the first two subsections we develop an alternative method to integrate $\log\theta_0(u)$ and $\log\Gamma_e(u)$, using certain series expansions that will be called (m,n) *representations*. We will often use the notion of a (m,n) *ray in the u-plane*, by which we mean a ray emanating from the origin, in direction of the vector $m\tau+n$ with $m\in\mathbb{N}$ and $n\in\mathbb{Z}$ In the last subsection we study the definition of the elliptic extensions Q from the perspective of (m,n) representations, thus obtaining a series representation for the even (in u) product of Q's. We end by briefly commenting upon an ambiguous overall phase function that appears in the definition of Q.

[26] The double zero at the origin splits into two single zeroes located at distances $\pm\frac{\epsilon}{2}$ from the origin along the dashed line in figure 9.

JHEP09(2020)184

Basic series representations. We start by presenting the representations that are building blocks of our forthcoming analysis. For θ_0 that representation is [35]

$$\log\theta_0(z;\tau) = -\mathrm{i}\sum_{j=1}^{\infty}\frac{\cos\big(j\pi(2z-\tau)\big)}{j\sin\pi j\tau}\,, \tag{C.1}$$

where the series on the right-hand side is absolutely convergent for

$$0 < \mathrm{Im}(z) < \mathrm{Im}(\tau)\,. \tag{C.2}$$

The analogous representation for elliptic Gamma functions is [35]

$$\log\Gamma_{\mathrm{e}}(z;\tau,\sigma) = -\frac{\mathrm{i}}{2}\sum_{j=1}^{\infty}\frac{\sin\big(j\pi(2z-\tau-\sigma)\big)}{j\sin\pi j\tau\sin\pi j\sigma}\,, \tag{C.3}$$

where the series on the right-hand side is absolutely convergent for

$$0 < \mathrm{Im}(z) < \mathrm{Im}(\tau) + \mathrm{Im}(\sigma)\,. \tag{C.4}$$

Some notation. In the presentation that follows we use the notation

$$z = z_{\perp\tau} + z_{\parallel\tau}\tau \tag{C.5}$$

for the real components of any complex number z along 1 and τ. This is very similar to the notation $z = z_1 + z_2\tau$ that we use in the main text, the difference being that here in (C.5) we consider τ to be variable, and so in particular we can replace τ by $m\tau + n$. We can write the components explicitly, for any τ and z, as

$$z_{\parallel\tau} = \frac{\mathrm{Im}\,z}{\tau_2}\,, \qquad z_{\perp\tau} = z - z_{\parallel\tau}\tau\,. \tag{C.6}$$

It is clear from definition (C.5) that

$$(z+k)_{\perp\tau} = z_{\perp\tau} + k\,, \qquad (kz)_{\perp\tau} = kz_{\perp\tau}\,, \qquad k\in\mathbb{R}\,. \tag{C.7}$$

The (m,n) representations of $\log\theta_0$

The series representation (C.1) implies the following formula,

$$\log\theta_0\left(\frac{z-k_0}{\tau};-\frac{1}{\tau}\right) = \mathrm{i}\sum_{j=1}^{\infty}\frac{\cos\big(\pi j\,\frac{2(z-k_0)+1}{\tau}\big)}{j\sin\frac{\pi j}{\tau}}\,, \tag{C.8}$$

which converges in the region

$$0 < \mathrm{Im}\left(\frac{z-k_0}{\tau}\right) < \mathrm{Im}\Big(-\frac{1}{\tau}\Big)\,. \tag{C.9}$$

Expanding z as in (C.5), we see that this convergence condition is equivalent to

$$0 < (-z+k_0)_{\perp\tau} < 1 \quad\Longrightarrow\quad 0 < -z_{\perp\tau} + k_0 < 1\,, \tag{C.10}$$

JHEP09(2020)184

where we have used (C.7) to reach the second set of inequalities. For $k_0 \in \mathbb{Z}$ the inequalities (C.10) are solvable if and only if $z_{\perp\tau} \notin \mathbb{Z}$. For fixed k_0 the region in the z-plane given by (C.10) is an infinite ribbon parallel to, and enclosing, the ray τ. The unique value of k_0 that satisfies this condition is,

$$k_0 = \lfloor z_{\perp\tau} \rfloor + 1 = -\lfloor -z_{\perp\tau} \rfloor \,. \tag{C.11}$$

The second equality in (C.11) follows from the fact that $z_{\perp\tau} \notin \mathbb{Z}$.

Now, combining the formula (C.8) with the modular transformation (A.22) we obtain, in the region (C.10),

$$\log \theta_0(z;\tau) = \pi \,\mathrm{i}\, B_{2,2}(z-k_0|\tau,-1) + \mathrm{i} \sum_{j=1}^{\infty} \frac{\cos\left(\pi j \,\frac{2(z-k_0)+1}{\tau}\right)}{j \sin \frac{\pi j}{\tau}} \,. \tag{C.12}$$

In exactly the same manner we can combine the basic series representations with the factorization formulas (A.27) to obtain, for any given (m,n),

$$\begin{aligned} \log \theta_0(z;\tau) = \pi \,\mathrm{i} \sum_{\ell=0}^{m-1} B_{2,2}(z - k_0(\ell,z) + \ell\tau | m\tau + n, -1) + \\ + \,\mathrm{i} \sum_{j=1}^{\infty} \frac{1}{j \sin \frac{\pi j}{m\tau+n}} \sum_{\ell=0}^{m-1} \cos\left(\pi j \,\frac{2(z-k_0(\ell,z)+\ell\tau)+1}{m\tau+n}\right) , \end{aligned} \tag{C.13}$$

which converges when the following condition is satisfied for $\ell = 0, \ldots, m-1$,

$$0 < \big(-z + k_0(\ell,z)\big)_{\perp m\tau+n} < 1 \quad \Longleftrightarrow \quad k_0(\ell,z) = -\lfloor (-z-\ell\tau)_{\perp m\tau+n} \rfloor \,. \tag{C.14}$$

Representations (C.13) will be called (m,n) representations of $\log\theta_0(z)$.

In what follows we will encounter the combination

$$u_2 \log \theta_0(z_I(u);\tau) - u_2 \log \theta_0(z_I(-u);\tau) \,, \tag{C.15}$$

where the index I stands for either chiral (C) or vector (V) multiplets, and

$$z_I(u) = u + \frac{r_I}{2}(2\tau+1) \,, \tag{C.16}$$

with r_I the R-charge of multiplet I.

Next, we will use representations (C.13) in both terms in (C.15), for which the choice of k_0 is

$$k_0(\ell, z_I(\pm u)) = -\Big\lfloor \mp u_{\perp m\tau+n} + \frac{d}{c}\,(r_I+\ell) - \frac{r_I}{2} \Big\rfloor \,, \tag{C.17}$$

when the argument of the function $\lfloor\ \rfloor$ is not an integer. We note that in the domain

$$|u_{\perp m\tau+n}| < \kappa(r_I,\, \ell,\, m,\, n) \,, \tag{C.18}$$

with

$$\kappa(r_I,\, \ell,\, m,\, n) = \min\Big(\Big\{ \frac{n}{m}\,(r_I+\ell) - \frac{r_I}{2} \Big\},\, 1 - \Big\{ \frac{n}{m}\,(r_I+\ell) - \frac{r_I}{2} \Big\} \Big) \,, \tag{C.19}$$

JHEP09(2020)184

and for

$$\frac{n}{m}\,(r_I+\ell)-\frac{r_I}{2}\notin\mathbb{Z}\,, \tag{C.20}$$

the functions $k_0(\ell, z_I(u))$ and $k_0(\ell, z_I(-u))$ are both equal to

$$k_0(\ell)=-\Big\lfloor\,\frac{n}{m}\,(r_I+\ell)-\frac{r_I}{2}\,\Big\rfloor\,, \tag{C.21}$$

and, in particular, they are independent of u.

Each value of R-charge r_I defines the width of the ribbon-like domain of absolute convergence (C.18). The middle axis of this ribbon passes through the origin of u-plane, and is parallel to the vector $m\tau+n$. For a theory with various building-block multiplets, we linearly combine the (m,n) representations of (C.15). The domain of absolute convergence of the (m,n) representation of such linear combinations is typically determined by the R-charge of one of the building-block multiplets. For instance, we can ask for the domain of absolute convergence of the $(c,0)$ representation of a linear combination of terms like (C.15), associated to $\mathcal{N}=4$ SYM, for which the spectrum of R-charges is $r_V=2$ and $r_C=\frac{2}{3}$. For that case, from equality $\kappa(r_V,\ell,m,0)=0$ and (C.18), it follows that the domain of absolute convergence of the latter linear combination of $(m,0)$ representations is *empty*. To deal with this issue we use the infinitesimal regulator $\epsilon=0^+$ that was introduced in [14] and mentioned in appendix B. For the vector and chiral multiplets, such regulator is introduced as the following infinitesimal deformation of the R-charge spectrum, $r_V=2-\epsilon$ and $r_C=\frac{2+\epsilon}{3}$. In that case, the $(c,0)$-representation of the corresponding linear combination of (C.15) is absolutely convergent in $|u_{\perp c\tau}|<\frac{\epsilon}{2}=0^+$, i.e., in a ribbon of infinitesimal width ϵ directed along the $(1,0)$-ray.

To summarize, after using the formula (C.13) we obtain the following absolutely convergent series representation in the domain (C.18) and for the choice of $k_0(\ell)$ given in (C.21),

$$\begin{aligned} &u_2\,\log\theta_0(z_I(u);\tau)-u_2\,\log\theta_0(z_I(-u);\tau)\\ &\qquad=2\,\mathcal{F}'^{(m,n)}(u)+\sum_{j=1}^{\infty}\frac{2}{j}\,c_2'(j;m,n)\,u_2\sin\frac{2\pi\,j\,u}{m\tau+n}\,. \end{aligned} \tag{C.22}$$

Here the pre-factor $\mathcal{F}'^{(m,n)}(u)$ is

$$2\,\mathcal{F}'^{(m,n)}(u)=\pi\,\mathrm{i}\sum_{\ell=0}^{m-1}\Big(u_2\,B_{2,2}(z_I(u)-k_0(\ell)+\ell\tau|\,m\tau+n,-1)+(u\to-u)\Big)\,, \tag{C.23}$$

and

$$c_2'(j;m,n)=-\,\mathrm{i}\sum_{\ell=0}^{m-1}\frac{\sin\frac{\pi\,j\,(r_I(2\tau+1)+1-2k_0(\ell)+2\ell\tau)}{m\tau+n}}{\sin\frac{\pi j}{m\tau+n}}\,. \tag{C.24}$$

From an explicit expansion of (C.23) for several values of m, n, and R-charge r_I, we have checked that for values of u in an (m,n) ray i.e for $u=\frac{u_2}{m}(m\tau+n)$ the quantity

$$2\,\mathcal{F}'^{(m,n)}(u)+2\pi\mathrm{i}\,(2r_I-1)\,u_2^2\,\tau \tag{C.25}$$

JHEP09(2020)184

$m \setminus n$	0	1	2	3	4	5	6	7	8	9	10
1	0	-4	-10	-10	-16	-22	-22	-28	-34	-34	-40
2	0	$\square$	-4	-6	-10	-9	-10	-15	-16	-18	-22
3	0	$-\frac{4}{3}$	$-\frac{8}{3}$	-4	$-\frac{14}{3}$	$-\frac{20}{3}$	-10	$-\frac{26}{3}$	$-\frac{32}{3}$	-10	$-\frac{38}{3}$
4	0	$-\frac{3}{2}$	$\square$	$-\frac{5}{2}$	-4	$-\frac{11}{2}$	-6	-7	-10	$-\frac{17}{2}$	-9
5	0	$-\frac{2}{5}$	$-\frac{8}{5}$	$-\frac{12}{5}$	$-\frac{18}{5}$	-4	$-\frac{24}{5}$	-6	-6	$-\frac{36}{5}$	-10
6	0	$-\frac{2}{3}$	$-\frac{4}{3}$	$\square$	$-\frac{8}{3}$	$-\frac{10}{3}$	-4	$-\frac{13}{3}$	$-\frac{14}{3}$	-6	$-\frac{20}{3}$
7	0	$-\frac{6}{7}$	$-\frac{6}{7}$	$-\frac{12}{7}$	$-\frac{16}{7}$	$-\frac{22}{7}$	$-\frac{22}{7}$	-4	$-\frac{34}{7}$	$-\frac{34}{7}$	$-\frac{40}{7}$
8	0	$-\frac{1}{4}$	$-\frac{3}{2}$	$-\frac{7}{4}$	$\square$	$-\frac{9}{4}$	$-\frac{5}{2}$	$-\frac{15}{4}$	-4	$-\frac{9}{2}$	$-\frac{11}{2}$
9	0	$-\frac{4}{9}$	$-\frac{10}{9}$	$-\frac{4}{3}$	$-\frac{16}{9}$	$-\frac{20}{9}$	$-\frac{8}{3}$	$-\frac{26}{9}$	$-\frac{32}{9}$	-4	$-\frac{38}{9}$
10	0	$-\frac{3}{5}$	$-\frac{2}{5}$	$-\frac{6}{5}$	$-\frac{8}{5}$	$\square$	$-\frac{12}{5}$	$-\frac{14}{5}$	$-\frac{18}{5}$	$-\frac{17}{5}$	-4

Table 3. Table of values of $\eta'(m,n)$. Notice that $m^2\,\eta'$ is always an integer and that η' only depends on the combination n/m. The squared boxes mark the slots corresponding to pairs (m,n) that are proportional to the pair $(2,1)$ for which the regulator ϵ fails (see the last paragraph of appendix B).

is purely imaginary and is independent of τ. After summing (C.25) over the matter content of $\mathcal{N}=4$ SYM, and taking the regulator ϵ to zero, one obtains

$$\sum_I 2\,\mathcal{F}'^{(m,n)}(u) + 8\pi\mathrm{i}\,u_2^2\,\tau = 2\pi\mathrm{i}\,u_2^2\,\eta'(m,n)\,, \tag{C.26}$$

where η' is a real function. The index I runs over the labels of vector and three chiral multiplets of $\mathcal{N}=4$ SYM, each of them with their corresponding charge asignment r_I. We have checked the following three properties in numerous examples (not proven): (a) that the coefficient $\eta'(m,n)$ is rational, (b) that it depends only on the ratio n/m, and (c) that $m^2\,\eta'(m,n) \in \mathbb{Z}$ (see table 3).

The (m,n) representations of $\log\Gamma_{\mathrm{e}}(z;\tau,\tau)$

We now develop similar series representations for the function $\log\Gamma_{\mathrm{e}}(z;\tau,\tau)$ using the basic series representation (C.3) for $\log\Gamma_{\mathrm{e}}(z;\tau,\sigma)$ and the modular factorization identities (A.29). We start with an identity analogous to (C.12) for the Γ_{e}-function by combining (C.3) with the basic modular identity (A.24). The locus $\sigma=\tau$, however, is not in the range of validity of (A.24), so we need to take a limit $\sigma\to\tau$. After substituting the two elliptic gamma functions in the right-hand side of (A.24) by their respective series representations (C.3) and taking the limit $\varepsilon\to 0$ with $\sigma=\tau+\varepsilon$ in the resulting expressions, one obtains the

JHEP09(2020)184

following representation, for any $k_0 \in \mathbb{Z}$,

$$\begin{aligned}\log\Gamma_{\rm e}(z;\,\tau,\,\tau) = \frac{\pi i}{3} B_{3,3}(z-k_0|\tau,\tau,-1) \\ + \,\mathrm{i}\left(\sum_{j=1}^{\infty} \frac{-2\,\tau+2(z-k_0)+1}{2\,j\,\tau\,\sin\left(\frac{\pi j}{\tau}\right)}\,\cos\frac{\pi j(2(\,z-k_0)+1)}{\tau}\right. \\ \left. -\,\frac{\pi j\cot\left(\frac{\pi j}{\tau}\right)+\tau}{2\pi\,j^2\,\tau\,\sin\left(\frac{\pi j}{\tau}\right)}\,\sin\frac{\pi j(2(z-k_0)+1)}{\tau}\right).\end{aligned} \tag{C.27}$$

From domain of convergence of the series (C.3), given in (C.4), it follows that the series on the right-hand side of (C.27) are absolutely convergent in $0 < -z_{\perp\tau} + k_0 < 1$. We have numerically checked the veracity of (C.27) in this ribbon, using the defining product representation (2.15) of the $\Gamma_{\rm e}$-function. From representations (C.27) and the factorization property (A.28), one obtains the following representations

$$\begin{aligned}\log\Gamma_{\rm e}(z;\tau,\tau) = \sum_{\ell=0}^{2(m-1)} \frac{\pi i}{3} B_{3,3}(z+\ell\tau-k_0|m\tau+n,m\tau+n,-1) \\ +\sum_{\ell=0}^{2(m-1)}\mathrm{i}\left(\sum_{j=1}^{\infty}\frac{-2(m\tau+n)+2(z+\ell\tau-k_0)+1}{2j(m\tau+n)\sin\left(\frac{\pi j}{m\tau+n}\right)}\cos\frac{\pi j(2(z+\ell\tau-k_0)+1)}{m\tau+n}\right. \\ \left. -\frac{\pi j\cot\left(\frac{\pi j}{m\tau+n}\right)+(m\tau+n)}{2\pi j^2(m\tau+n)\sin\left(\frac{\pi j}{m\tau+n}\right)}\sin\frac{\pi j(2(z+\ell\tau-k_0)+1)}{m\tau+n}\right).\end{aligned} \tag{C.28}$$

We call them (m,n) representations of $\log\Gamma_{\rm e}(z;\tau,\tau)$. Since our eventual goal is to use these formulas to represent the SYM index, wherein only even combinations of $\log\Gamma_{\rm e}(z_I(u);\tau,\tau)$ appear, we move directly to a representation of such functions which will be very useful for us in the following. For every (m,n),

$$\begin{aligned}&\log\Gamma_{\rm e}(z_I(u);\tau,\tau)+\log\Gamma_{\rm e}(z_I(-u);\tau,\tau) = \\ &-\,2\,\mathcal{F}^{(m,n)}(u)\,+\sum_{j=1}^{\infty}\frac{2}{j}\Big(c_1(j;m,n)\,g(ju;m\tau+n)+c_2(j;c,d)\,\widehat{g}(j;u,m\tau+n)\Big)\,,\end{aligned} \tag{C.29}$$

which follows from the identity (C.28) and the definition (C.16). Analogously to the (m,n) representations (C.22), the series in the right-hand side of (C.28) and (C.29) are absolutely convergent in domain (C.18) for the $k_0(\ell)$ in (C.21). In figure 10 we have plotted the real part of a couple of series representations (C.29) and compared them with the representation of the left-hand side of (C.29) that one obtains after using the product definition of $\log\Gamma_{\rm e}(z;\tau,\tau)$.

The pre-factor $\mathcal{F}^{(m,n)}(u)$ is defined as

$$-2\,\mathcal{F}^{(m,n)}(u) = \frac{\pi\,\mathrm{i}}{3}\sum_{\ell=0}^{2(m-1)}(m-|\ell-m+1|)\Big(B_{3,3}\big(z_I(u)-k_0(\ell)+\ell\tau|m\tau+n,m\tau+n,-1\big)+(u\to-u)\Big)\,. \tag{C.30}$$

JHEP09(2020)184

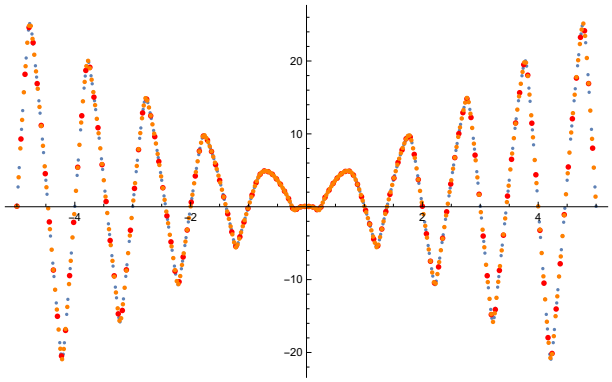

Figure 10. The numerical plots of $\log\left|\prod_I \Gamma_{\rm e}(z_I(u(\upsilon));\,\tau,\,\tau)\Gamma_{\rm e}(z_I(-u(\upsilon));\,\tau,\,\tau)\right|$ as a function of $\upsilon\in\mathbb{R}$, for $\tau=1+2\,\mathrm{i}$ and $u(\upsilon)=\upsilon\,\tau$. The blue points are obtained by using the product representation (2.15) with $\epsilon=0.2$. We have truncated this representation at level $j+k=30$, where the indices j and k are the mute ones in the product (2.15). The orange points are obtained by using (C.29) for $m=2$, $n=0$, $\epsilon=0.2$. We truncate this series at level $j=30$, where the index j is the mute one in the $(2,0)$ representation (C.29). The red points are obtained by using the representation (C.29) with $m=1$, $n=0$, and $\epsilon=0.2$. We truncate this series at level $j=30$, where the index j is the mute one in the $(1,0)$ representation (C.29).

The function $g(u;\tau)$ (which is periodic under $u\mapsto u+\tau$) and the function $\widehat{g}(u;\tau)$ (which is not periodic under this shift) are

$$g(u;\tau)=\cos\frac{2\pi u}{\tau}\,,\qquad \widehat{g}(j;u,\tau)=\frac{u}{\tau}\,\sin\frac{2\pi j u}{\tau}\,, \tag{C.31}$$

and the series coefficients in (C.29) are

$$\begin{aligned} c_1(j;m,n)=&-\frac{\mathrm{i}}{2}\sum_{\ell=0}^{2(m-1)}(m-|\ell-m+1|)\times \\ &\times\left(\frac{\cos\frac{\pi j}{m\tau+n}+\frac{m\tau+n}{\pi j}\sin\frac{\pi j}{m\tau+n}}{(m\tau+n)\sin^2\frac{\pi j}{m\tau+n}}\,\sin\left(\frac{\pi j(r_I(2\tau+1)-2k_0(\ell)+2\ell\tau+1)}{m\tau+n}\right)\right. \\ &\left.-\frac{\left(-2(m\tau+n)+r_I(2\tau+1)-2k_0(\ell)+2\ell\tau+1\right)}{(m\tau+n)\sin\frac{\pi j}{m\tau+n}}\,\cos\left(\frac{\pi j(r_I(2\tau+1)-2k_0(\ell)+2\ell\tau+1)}{m\tau+n}\right)\right), \end{aligned} \tag{C.32}$$

and

$$\begin{aligned} c_2(j;m,n)&=-\,\mathrm{i}\sum_{\ell=0}^{2(m-1)}(m-|\ell-m+1|)\,\frac{\sin\frac{\pi j(r_I(2\tau+1)-2k_0(\ell)+2\ell\tau+1)}{m\tau+n}}{\sin\frac{\pi j}{m\tau+n}} \\ &=-\,\mathrm{i}\,m\sum_{\ell=0}^{m-1}\frac{\sin\frac{\pi j(r_I(2\tau+1)-2k_0(\ell)+2\ell\tau+1)}{m\tau+n}}{\sin\frac{\pi j}{m\tau+n}}\,. \end{aligned} \tag{C.33}$$

In going from the first to the second line in (C.33) we have used the identity $k_0(\ell+m)=k_0(\ell)-n$ (which follows immediately from (C.21)), and the identity

$$(m-|\ell-m+1|)+(m-|\ell+1|)=m\,, \tag{C.34}$$

which is valid for $0\le\ell<m$.

JHEP09(2020)184

$m \setminus n$	0	1	2	3	4	5	6	7	8	9	10
1	0	0	-1	1	0	-1	1	0	-1	1	0
2	0	$\square$	0	0	-1	$\frac{1}{2}$	1	$-\frac{1}{2}$	0	0	-1
3	0	0	0	0	$\frac{1}{3}$	0	-1	$\frac{1}{3}$	0	1	$\frac{1}{3}$
4	0	$-\frac{1}{4}$	$\square$	$\frac{1}{4}$	0	$-\frac{1}{4}$	0	0	-1	$\frac{1}{4}$	$\frac{1}{2}$
5	0	$\frac{1}{5}$	0	0	$-\frac{1}{5}$	0	0	$-\frac{1}{5}$	$\frac{1}{5}$	0	-1
6	0	0	0	$\square$	0	0	0	$\frac{1}{6}$	$\frac{1}{3}$	0	0
7	0	$-\frac{1}{7}$	$\frac{1}{7}$	0	0	$-\frac{1}{7}$	$\frac{1}{7}$	0	$-\frac{1}{7}$	$\frac{1}{7}$	0
8	0	$\frac{1}{8}$	$-\frac{1}{4}$	$-\frac{1}{8}$	$\square$	$\frac{1}{8}$	$\frac{1}{4}$	$-\frac{1}{8}$	0	0	$-\frac{1}{4}$
9	0	0	$-\frac{1}{9}$	0	0	0	0	$\frac{1}{9}$	0	0	$\frac{1}{9}$
10	0	$-\frac{1}{10}$	$\frac{1}{5}$	0	0	$\square$	0	0	$-\frac{1}{5}$	$\frac{1}{10}$	0

Table 4. Table of values of $\eta(m,n)$. Note that $m^2\,\eta(m,n)$ is always integer and that $\eta(m,n)$ is only a function of the quotient $\frac{n}{m}$. The squared boxes mark the slots corresponding to pairs (m,n) that are proportional to the pair $(2,1)$ for which the regulator ϵ fails (see the last paragraph of appendix B).

For u along an (m,n) ray i.e. $u = \frac{u_2}{m}(m\tau + n)$, and several values of m, n and R-charges r_I, we have checked that the quantity

$$-2\,\mathcal{F}^{(m,n)}(u) + 2\,\mathcal{F}^{(m,n)}(0) + 2\pi\mathrm{i}\,\tau\,u_2^2\,(r_I - 1)\,, \tag{C.35}$$

is purely imaginary. After summing (C.35) over the matter content of $\mathcal{N}=4$ SYM, and taking the regulator ϵ to zero, one obtains

$$-2\sum_I \mathcal{F}^{(m,n)}(u) + 2\sum_I \mathcal{F}^{(m,n)}(0) = 2\pi\mathrm{i}\,\eta(m,n)\,(u_2)^2\,. \tag{C.36}$$

Before moving on, let us comment briefly about the constant $\eta(m,n)$. As for η' we have checked the following three properties of $\eta(m,n)$ in numerous examples: (a) it is rational, (b) it depends only on the ratio n/m, and (c) $m^2\,\eta(m,n) \in \mathbb{Z}$ (see table 4). The last property will be useful in the next appendix.

The (m,n) representations of the elliptic extension

In section 3 we showed that although $\Gamma_{\rm e}(u)$ is not elliptic invariant one can dress it with $\theta_0(u)^{u_2}$ to produce the elliptic function $Q^{-1}(u)$ that coincides with $\Gamma_{\rm e}(u)$ at $u_2 = 0$, and is holomorphic in τ for finite values of u_2. The function Q was represented by the double Fourier series expansion (3.20) which includes the τ-independent purely imaginary term $\mathrm{i}\Psi$ which was not fixed. In this subsection, we find an alternate representation of the even-in-u product (from now even product) of Q's that follows from the (m,n) representations of θ_0 and $\Gamma_{\rm e}$ that we have developed in the previous appendices. As before, we work with the even combination $\Gamma_{\rm e}(z_I(u);\tau,\tau)\,\Gamma_{\rm e}(z_I(-u);\tau,\tau)$ appearing in the index formula.

JHEP09(2020)184

We show that, along an (m,n) ray, the even product of Q's, coincides with the (m,n) representation of the even product of $\Gamma_{\rm e}$'s, once the non-periodic part $\widehat{g}$ of the $\Gamma_{\rm e}$'s is projected out.[27] We end this section by using this result to deduce an identity that will be used in section E to relate the elliptic and meromorphic actions of (m,n) configurations.

We start by proving a useful identity. Upon comparing the coefficient of the third term in (C.29) with the coefficient of the second term in (C.22), we conclude that along an (m,n) ray i.e. for $u=\frac{u_2}{m}(m\tau+n)$,

$$\begin{aligned}\sum_{j=1}^{\infty}\frac{2}{j}\,c_2(j;m,n)\,\widehat{g}(j;u,m\tau+n)&=\sum_{j=1}^{\infty}\frac{2}{j}\,c_2'(j;m,n)\,u_2\,\sin\frac{2\pi\,j\,u}{m\tau+n}\\&=u_2\,\log\theta_0(z_I(u);\tau)-u_2\,\log\theta_0(z_I(-u);\tau)-2\,\mathcal{F}^{\prime(m,n)}(u)\,.\end{aligned}\tag{C.37}$$

We are ready to reach an (m,n) representation for the logarithm of the even product of the function Q defined in (3.21). More specifically, we focus on the logarithm of the object in the left-hand side of

$$\begin{aligned}\frac{1}{Q_{\left(r_I-1,\,\frac{r_I}{2}\right)}(u)Q_{\left(r_I-1,\,\frac{r_I}{2}\right)}(-u)}&=\mathbf{e}\big(\widetilde{\Psi}(u)\big)\,\mathbf{e}\big(-r_I\,\tau\,u_2^2\big)\\&\quad\times\frac{\Gamma_{\rm e}(z_I(u);\tau,\tau)\Gamma_{\rm e}(z_I(-u);\tau,\tau)}{\theta_0(z_I(u);\tau)^{u_2}\theta_0(z_I(-u);\tau)^{-u_2}}.\end{aligned}\tag{C.38}$$

The τ-independent function $\widetilde{\Psi}(u)$ is a real-analytic, perhaps multi-valued, function obeying the following two conditions. Firstly, it needs to obey the initial condition

$$\widetilde{\Psi}(u_2=0)=0\tag{C.39}$$

so that the left-hand side of (C.38) reduces to $\Gamma_{\rm e}(z_I(u_1))\Gamma_{\rm e}(z_I(-u_1))$ for $u_2=0$. Secondly, its "lack of ellipticity" needs to be such that (C.38) is an elliptic function in u-plane.

Finally, we move on to write down the (m,n) representation of the logarithm of (C.38).[28] We will do so in three steps. First, we define such logarithm, using representations (C.22) and (C.29). For $u=\frac{u_2}{m}(m\tau+n)$ one obtains

$$\begin{aligned}&-\log Q_{\left(r_I-1,\,\frac{r_I}{2}\right)}(u)-\log Q_{\left(r_I-1,\,\frac{r_I}{2}\right)}(-u)\\&=2\pi\mathrm{i}\,\big(\,\widetilde{\Psi}(u)-\tau\,r_I\,u_2^2\,\big)-2\,\mathcal{F}^{(m,n)}(u)\;-\;2\,\mathcal{F}^{\prime(m,n)}(u)+\sum_{j=1}^{\infty}\frac{2}{j}c_1(j;m,n)\,g(ju;m\tau+n)\,.\end{aligned}\tag{C.40}$$

Second, before reaching the final equation, we must note an interesting property. Representations (C.40) are labelled by $m\in\mathbb{N}$ and $n\in\mathbb{Z}$. From observations made on expressions (C.25) and (C.35), it follows that, along an (m,n) ray i.e. for $u=\frac{u_2}{m}(m\tau+n)$

$$\begin{aligned}&-2\pi\mathrm{i}\,\tau\,r_I\,u_2^2-2\,\mathcal{F}^{(m,n)}(u)\;-\;2\,\mathcal{F}^{\prime(m,n)}(u)\\&\qquad=-\,2\,\mathcal{F}^{(m,n)}(0)+2\pi\mathrm{i}\,\big(\eta(m,n)-\eta'(m,n)\big)\,u_2^2.\end{aligned}\tag{C.41}$$

[27] Recall that the series (C.29) has three parts the pre-factor $\mathcal{F}$, the periodic part (governed by $g(n\,u;\tau)$), and the non-periodic part ($\widehat{g}(n\,u;\tau)$).

[28] Before entering into definition of logarithms, it worths noticing that the $\theta_0(z_I(\pm u))^{\pm u_2}$ in the right-hand side of (C.38) must be defined with care, as the power function is multivalued when acting over the field of complex numbers (except for integer powers).

JHEP09(2020)184

The second term in the second line is a τ-independent imaginary term proportional to u_2^2. Third, and final, we plug (C.41) in (C.40) and redefine $\widetilde{\Psi}(u) \to \widetilde{\Psi}(u) - (\eta(m,n) - \eta'(m,n))\, u_2^2$, so that, for all $m \in \mathbb{N}$ and $n \in \mathbb{Z}$, and for $u = \frac{u_2}{m}(m\tau + n)$

$$\begin{aligned} &- \log Q_{\left(r_I - 1, \frac{r_I}{2}\right)}(u) - \log Q_{\left(r_I - 1, \frac{r_I}{2}\right)}(-u) \\ &\qquad = 2\pi \mathrm{i}\, \widetilde{\Psi}(u) - 2\, \mathcal{F}^{(m,n)}(0) + \sum_{j=1}^{\infty} \frac{2}{j}\, c_1(j;m,n)\, g(ju; m\tau + n)\,. \end{aligned} \tag{C.42}$$

This is the (m,n) representation we were looking for. It shows that along an (m,n) ray, the even sum of elliptic functions $-\log Q$ in the left-hand side, can be seen, up to a redefinition of $\widetilde{\Psi}(u)$,[29] as the result of projecting out the non periodic part $\widetilde{g}$ in (m,n) representation (C.29) of the corresponding even sum of $\log \Gamma_{\mathrm{e}}$. Notice that $\widetilde{\Psi}(u)$ in (C.42) is still ambiguous, but it is elliptic, satisfies (C.39), and it does not depend on τ.

Equation (C.42) and the definition of the elliptic extension of the action $S(\underline{u})$ given in (3.26), implies the following identity

$$S_{\mathrm{eff}}(m,n;\tau) = N^2 \sum_I \mathcal{F}^{(m,n)}(0) + \pi \mathrm{i} N^2 \widetilde{\varphi}(m,n)\,, \tag{C.43}$$

where $\frac{\widetilde{\varphi}(m,n)}{4} \in \mathbb{R}$ are the Fourier coefficients of $\widetilde{\Psi}(u)$ along the (m,n) ray. They are arbitrary constants that could be matched to $\varphi(m,n)$. We have checked that the right-hand side of (C.43) coincides with the right-hand side of (4.13) for several values of $m \in \mathbb{N}$, $n \in \mathbb{Z}$ and $\gcd(m,n) = 1$. This will be used in section E to match the elliptic and meromorphic actions (up to a τ-independent imaginary quantity).

D The role of the saddle $(0,0)$

We now clarify the role (and the lack of role) of the saddle $(0,0)$. First let's turn off the regulator ϵ so that $u_i = 0$ strictly. In this case the vector multiplet has $z_V(0) = 2\tau + 1$ (see equation (C.16)). From the product representation (2.15) we see that this value of z_V is a zero of the elliptic gamma function and therefore the index actually vanishes. Now let's turn on the regulator ϵ. From the representation (C.29) we see that, for small enough ϵ for fixed $\tau \in \mathbb{H}$, the quantity $-\mathrm{Re}\, S(0,0)$ is negative and thus the contribution of saddle $(0,0)$ is suppressed. These observations are summarized in figure 11. For the $(0,0)$ saddle, all values of (m,n) in the representation (C.29) clearly give the same answer. We have used $m = 1$, $n = 0$ to generate the figure.

In contrast, for fixed ϵ and in the Cardy-like limit ($\tau \to 0$ with $\tau_1 < 0$) the quantity $-\mathrm{Re}\, S(0,0)$ becomes positive. Furthermore, as shown in [14], the full action asymptotes to the action of the black hole. In section 4.5 we have revisited and confirmed the results of [14], as to how any asymptotic limit $\tau \to 0$ of the action of the black hole saddle $(1,0)$ coincides, in that very same limit, with the ϵ-regulated action of the $(0,0)$ saddle.

[29] The new $\widetilde{\Psi}$ is doubly periodic, respects the constraint (C.39), and is real-valued.

JHEP09(2020)184

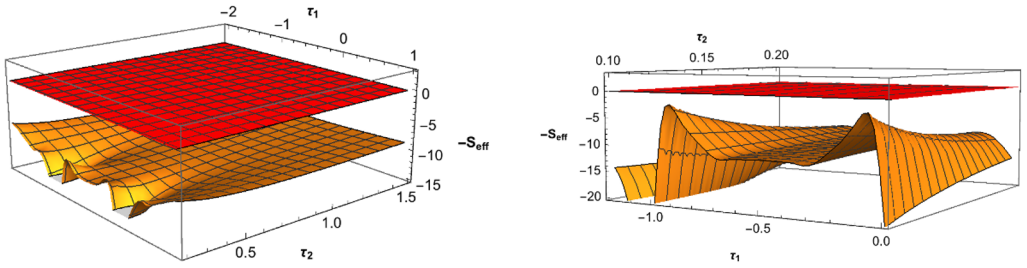

Figure 11. $-\mathrm{Re}\, S(0,0)$ (Orange) vs $-\mathrm{Re}\, S(0,1) = 0$ (Red). The unit of the vertical axis is $\frac{N^2}{2}$. We have used the representation (C.29) with $m = 1$ and $n = 0$, with a truncation at $j = 2000$. The plot on the left covers the domain $\tau_1 \in [-2,\, 1]$ and $\tau_2 \in [0.2,\, 1.5]$, and the plot on the right covers the domain $\tau_1 \in [-1.2,\, 0]$ and $\tau_2 \in [0.1,\, 0.2]$. Both plots have $\epsilon = 0.001$ which is small enough for the ranges of τ considered here, so that the $(0,0)$ solution is suppressed with respect to $(0,1)$.

E The (m,n) meromorphic action

In this appendix we evaluate the analytic continuation of the integrand of (2.16) on the (m,n) configurations $u_i = (m\tau + n)\frac{i}{N}$ and compare it with the valuation of the elliptic extension of the action calculated in section 4 on the same configurations. To ease the language, we will call the negative of the logarithm of these two quantities, the *meromorphic action* and the *elliptic action*, respectively. We find that, remarkably, although the (m,n) configurations are not saddles of the meromorphic action, the *valuations* of the meromorphic and elliptic actions on these configurations are essentially the same![30]

The meromorphic action is defined as the logarithm of the integrand of (2.16) at large N, i.e. (the relevant notation has been summarized near (C.16)),

$$S_{\text{mero}}(\underline{u}) := -\sum_I \sum_{i,j} \log\Gamma_{\text{e}}\left(u_{ij} + \frac{r_I}{2}(2\tau+1);\tau,\tau\right). \tag{E.1}$$

In particular, using the regulator discussed in the previous appendix, we should take $r_V = 2-\epsilon$ and $r_C = \frac{2+\epsilon}{3}$, and $\epsilon \to 0^+$ at the end.

In order to calculate the meromorphic action we simply evaluate the series representation of the elliptic gamma functions developed in the previous section on the $(m,\, n)$ configuration,

$$u_{ij} = (m\tau + n)\,\frac{i-j}{N}\,. \tag{E.2}$$

We recall that the (m,n) series representation (C.29) has three parts, the pre-factor $\mathcal{F}$, the periodic part (governed by $g(j\,u;\tau)$), and the non-periodic part ($\widehat{g}(j\,u;\tau)$). We proceed to evaluate them on the configuration (E.2).

From the identity,

$$\sum_{i,\,j=1}^{N} g\left(k_1(m\tau+n)\frac{i-j}{N};\, m\,\tau+\,n\right) = \sum_{k_2\in\mathbb{Z}} N^2\,\delta_{k_1,\,k_2\,N}\,, \tag{E.3}$$

[30]The difference of the two actions is a purely imaginary τ-independent term, that depends on m and n.

JHEP09(2020)184

it follows that the only non-vanishing contributions in the series

$$\sum_{k=1}^{\infty} \frac{1}{k}\, c_1(k;m,n) \sum_{i,\,j=1}^{N} g\left(k(\,m\tau+n\,)\frac{(i-j)}{N};\, m\,\tau+n\right) \tag{E.4}$$

are when k equals integer multiples of N. Noting that the coefficients $c_1(k;m,n)$ (C.32) are exponentially suppressed as a function of k for large k, we have that the double sum (E.4) behaves like e^{-N} and therefore vanishes in the large-N limit.

The non-periodic function $\widehat{g}(u;m\tau+n)$ vanishes as well when evaluated on (E.2). This follows from the identity, $k\in\mathbb{Z}$,

$$\sum_{i,\,j=1}^{N}\left(\frac{i-j}{N}\right)\sin\left(\frac{2\pi k(i-j)}{N}\right)=0\,, \tag{E.5}$$

which is proved as follows

$$\begin{aligned}\sum_{i,j=1}^{N}(i-j)\,\mathbf{e}\big(\tfrac{i-j}{N}k\big) &= \sum_{i=1}^{N} i\,\mathbf{e}\big(\tfrac{i}{N}k\big)\sum_{j=1}^{N}\mathbf{e}\big(\tfrac{-j}{N}k\big)-\sum_{j=1}^{N} j\,\mathbf{e}\big(\tfrac{-j}{N}k\big)\sum_{i=1}^{N}\mathbf{e}\big(\tfrac{i}{N}k\big)\\ &= \sum_{i=1}^{N} i\,\mathbf{e}\big(\tfrac{i}{N}k\big)\,\delta_{k,0}-\sum_{j=1}^{N} j\,\mathbf{e}\big(\tfrac{-j}{N}k\big)\,\delta_{k,0}\\ &= \delta_{k,0}\left(\sum_{i=1}^{N} i-\sum_{j=1}^{N} j\right)=0\,.\end{aligned} \tag{E.6}$$

The only term contributing to the action (E.8) is the pre-factor $\mathcal{F}$. Using Formula (C.36), summing over all the $\Gamma_{\rm e}$-functions that contribute to the index, and using the fact that on the (m,n) ansatz

$$\sum_{i,j=1}^{N}(u_{ij\,2})^2=m^2\,\frac{\sum_{i,j=1}^{N}(i-j)^2}{N^2}=\frac{m^2}{6}(N^2-1)=\frac{m^2}{6}\,N^2+O\left(\frac{1}{N}\right), \tag{E.7}$$

we obtain that the value of the meromorphic action $S_{\rm mero}(\underline{u})$ on the (m,n) configuration is

$$S_{\rm eff}^{\rm mero}(m,n;\tau)=N^2\sum_{I}\mathcal{F}^{(m,n)}(0)-\frac{\pi\,\mathrm{i}}{6}\,N^2\,m^2\,\eta(m,n)\,, \tag{E.8}$$

where $\mathcal{F}^{(m,n)}(0)$ is defined by (C.30), and the index I runs over the matter content of $\mathcal{N}=4$ SYM. The real function $\eta(m,n)$ is the pure imaginary term discussed in (C.36).

Upon comparing the formulas (E.8) and (C.43), it follows that the elliptic and meromorphic (m,n) effective actions, for relatively prime (m,n), coincide up to a τ-independent imaginary quantity. Thus, for every coprime (m,n), the meromorphic action (E.8) can be

JHEP09(2020)184

written in the form[31]

$$S_{\text{eff}}^{\text{mero}}(m,n;\tau) = \frac{N^2\,\pi\,\mathrm{i}}{27\,m}\,\frac{\big(2(m\tau+n)+\chi_1(m+n)\big)^3}{(m\tau+n)^2} + N^2\,\pi\,\mathrm{i}\,\varphi_{\text{mero}}(m,n)\,, \tag{E.9}$$

where $\varphi_{\text{mero}}(m,n) \in \mathbb{R}$. In particular we find that $\varphi_{\text{mero}}(1,0) = 0$ as mentioned below equation (4.28).

We end this section with a comment about a subtle issue regarding the comparison between the elliptic and meromorphic approaches. Recall from the discussion in section 2 that, for N prime, the saddles of the elliptic action are labelled by pairs (m,n) such that $\gcd(m,n)=1$. We could have chosen to reparameterize the saddle (m,n) as (km,kn), where k is any integer — even depending on m,n — and this would not have made any difference to the elliptic action because elliptic symmetry forces the action to be a function of the quotient n/m, and not of m and n independently. In the meromorphic approach, however, we find that the action is not a function of n/m only. In particular, we have checked in several examples that the first summand in the right-hand side of (E.8) only depends on the ratio n/m but the second summand in the right-hand side of (E.8) is not just a function of n/m. If we think of this reparameterization as a "local rescaling" of the space of saddles with a function $k(m,n)$, we are drawn to conclude that the meromorphic action is anomalous under such a local scale-reparametrization. The resolution of this puzzle is tied to a better understanding of the imaginary term in the action (see Footnote 14).

F Relation to the $\mathcal{N}=4$ SYM Bethe Ansatz formula

In this subsection we make contact with the approach of [7, 8]. The Bethe Ansatz formula in these papers, introduced in a related context in [22, 23], has the following form for the $\mathcal{N}=4$ SYM index,

$$\mathcal{I}_{BA} = \kappa_N \sum_{\underline{u}^\star \in \text{BAEs}} \mathcal{Z}(\underline{u}^\star)\,\mathcal{H}^{-1}(\underline{u}^\star)\,. \tag{F.1}$$

Here the function $\mathcal{Z}(\underline{u})$ is the analytic continuation in $\underline{u}$ of the integrand of the index (2.14) — which is precisely what we discussed in appendix E, i.e. in our language $\mathcal{Z}(\underline{u}) = \exp\big(-S_{\text{eff}}^{\text{mero}}(\underline{u})\big)$ defined in (E.1). The factor $\mathcal{H}^{-1}$ is a Jacobian factor which is subleading in $\frac{1}{N}$ compared to the effective action. The factor κ_N is precisely the pre-factor in the right-hand side of our equation (2.16), which is also sub-leading in $\frac{1}{N}$. The numbers $\underline{u}^\star = \{u_i^\star\}$, $i=1,\dots N$ entering the formula, called Bethe roots, are solutions to a set of algebraic equations called the Bethe Ansatz Equations (BAEs), and obey $\sum_i u_i^\star = 0$.

[31] For N not a prime, recall that there are other solutions along (m,n) rays denoted by $(K|m,n)$ with $K|N$, and for m, n co-prime. We can also compute their large-N action by similar methods to be

$$S_{\text{eff}}^{\text{mero}}(K|m,n) = S_{\text{eff}}^{\text{mero}}(m,n) - \frac{N^2}{K}\sum_{j=1}^{\infty}\frac{c_1(jK;m,n)}{j} + \tau\text{-independent phase}\,.$$

The gap between the actions of $(N|m,n) \equiv (m,n)$ and $(K|m,n)$ vanishes exponentially fast for large values of $K \sim N$ because the coefficient c_1 is exponentially suppressed for large values of its first argument (the ϵ-regulator is important to do such calculations). It would be interesting to understand the meaning of the large-N limits of these solutions.

JHEP09(2020)184

The BAEs are equations for the positions of poles of the integrand in a certain integral representation of the SYM index (which does not look a priori the same as (2.16)). These equations are of the form

$$\prod_{j=1}^{N} f(u^\star_{ij}) = 1\,, \qquad i = 1, \ldots, N\,, \tag{F.2}$$

where f is a certain combination of θ_0-functions. Solutions to these equations were found in [7, 60, 61] and, in particular, it was shown that the (m, n) configuration i.e. $u^\star_{ij} = \frac{i-j}{N}(m\tau + n)$ with $\gcd(m, n) = 1$ is a solution to the BAEs. It was also shown that the $(1, 0)$ configuration[32] has the same entropy as the AdS_5 black hole.

From our point of view, we notice that the logarithm of the BAEs (F.2) is precisely of the form (2.7) for some $V(u)$ that is even in u and double-periodic on the lattice generated by 1 and τ. Thus, in virtue of our discussion in section 2, it follows that all the (m, n) configurations discussed in this paper are Bethe roots. Further, from the discussion in appendix E, it follows that the action of these roots is given by the formula (E.9). As mentioned below that equation, it agrees with the elliptic action introduced in this paper evaluated at the same saddle, up to a τ-independent imaginary term.

References

[1] C. Romelsberger, *Counting chiral primaries in $N = 1$, $d = 4$ superconformal field theories*, *Nucl. Phys. B* **747** (2006) 329 [hep-th/0510060] [INSPIRE].

[2] J. Kinney, J.M. Maldacena, S. Minwalla and S. Raju, *An Index for 4 dimensional super conformal theories*, *Commun. Math. Phys.* **275** (2007) 209 [hep-th/0510251] [INSPIRE].

[3] S.M. Hosseini, K. Hristov and A. Zaffaroni, *An extremization principle for the entropy of rotating BPS black holes in AdS_5*, *JHEP* **07** (2017) 106 [arXiv:1705.05383] [INSPIRE].

[4] A. Cabo-Bizet, D. Cassani, D. Martelli and S. Murthy, *Microscopic origin of the Bekenstein-Hawking entropy of supersymmetric AdS_5 black holes*, *JHEP* **10** (2019) 062 [arXiv:1810.11442] [INSPIRE].

[5] S. Choi, J. Kim, S. Kim and J. Nahmgoong, *Large AdS black holes from QFT*, arXiv:1810.12067 [INSPIRE].

[6] S. Choi, C. Hwang, S. Kim and J. Nahmgoong, *Entropy Functions of BPS Black Holes in AdS_4 and AdS_6*, *J. Korean Phys. Soc.* **76** (2020) 101 [arXiv:1811.02158] [INSPIRE].

[7] F. Benini and P. Milan, *A Bethe Ansatz type formula for the superconformal index*, *Commun. Math. Phys.* **376** (2020) 1413 [arXiv:1811.04107] [INSPIRE].

[32] The conventions of [8] can be matched to the ones used in this paper under the identifications $\tau_{\text{here}} \leftrightarrow \tau_{\text{there}} - 1$, $\Delta_{1,2,3} = (2\tau_{\text{there}} - 1)/3$, and $\mathcal{I}_{\text{here}}(\tau_{\text{here}}, \tau_{\text{here}}; n_0 = -1) \leftrightarrow \mathcal{I}_{\text{there}}(\Delta_1, \Delta_2, \Delta_3, \tau_{\text{there}}, \tau_{\text{there}})$. This leads to the following map between saddles: $(m, n)_{\text{there}} \leftrightarrow (m, m + n)_{\text{here}}$.

JHEP09(2020)184

[8] F. Benini and P. Milan, *Black Holes in 4D $\mathcal{N} = 4$ Super-Yang-Mills Field Theory*, *Phys. Rev. X* **10** (2020) 021037 [arXiv:1812.09613] [INSPIRE].

[9] M. Suh, *On-shell action and the Bekenstein-Hawking entropy of supersymmetric black holes in AdS_6*, arXiv:1812.10491 [INSPIRE].

[10] M. Honda, *Quantum Black Hole Entropy from 4d Supersymmetric Cardy formula*, *Phys. Rev. D* **100** (2019) 026008 [arXiv:1901.08091] [INSPIRE].

[11] A. Arabi Ardehali, *Cardy-like asymptotics of the 4d $\mathcal{N} = 4$ index and AdS_5 blackholes*, *JHEP* **06** (2019) 134 [arXiv:1902.06619] [INSPIRE].

[12] A. Zaffaroni, *Lectures on AdS Black Holes, Holography and Localization*, 2, 2019 [arXiv:1902.07176] [INSPIRE].

[13] J. Kim, S. Kim and J. Song, *A 4d $N = 1$ Cardy Formula*, arXiv:1904.03455 [INSPIRE].

[14] A. Cabo-Bizet, D. Cassani, D. Martelli and S. Murthy, *The asymptotic growth of states of the 4d $\mathcal{N} = 1$ superconformal index*, *JHEP* **08** (2019) 120 [arXiv:1904.05865] [INSPIRE].

[15] A. Amariti, I. Garozzo and G. Lo Monaco, *Entropy function from toric geometry*, arXiv:1904.10009 [INSPIRE].

[16] D. Cassani and L. Papini, *The BPS limit of rotating AdS black hole thermodynamics*, *JHEP* **09** (2019) 079 [arXiv:1906.10148] [INSPIRE].

[17] F. Larsen, J. Nian and Y. Zeng, *AdS_5 black hole entropy near the BPS limit*, *JHEP* **06** (2020) 001 [arXiv:1907.02505] [INSPIRE].

[18] G. Kántor, C. Papageorgakis and P. Richmond, *AdS_7 black-hole entropy and 5D $\mathcal{N} = 2$ Yang-Mills*, *JHEP* **01** (2020) 017 [arXiv:1907.02923] [INSPIRE].

[19] J. Nahmgoong, *6d superconformal Cardy formulas*, arXiv:1907.12582 [INSPIRE].

[20] A. González Lezcano and L.A. Pando Zayas, *Microstate counting via Bethe Ansätze in the 4d $\mathcal{N} = 1$ superconformal index*, *JHEP* **03** (2020) 088 [arXiv:1907.12841] [INSPIRE].

[21] A. Lanir, A. Nedelin and O. Sela, *Black hole entropy function for toric theories via Bethe Ansatz*, *JHEP* **04** (2020) 091 [arXiv:1908.01737] [INSPIRE].

[22] C. Closset, H. Kim and B. Willett, *$\mathcal{N} = 1$ supersymmetric indices and the four-dimensional A-model*, *JHEP* **08** (2017) 090 [arXiv:1707.05774] [INSPIRE].

[23] C. Closset, H. Kim and B. Willett, *Seifert fibering operators in 3d $\mathcal{N} = 2$ theories*, *JHEP* **11** (2018) 004 [arXiv:1807.02328] [INSPIRE].

[24] S.J. Bloch, *Higher Regulators, Algebraic K-Theory, and Zeta Functions of Elliptic Curves*, CRM Monograph Series, vol. 11 (2000).

[25] D. Zagier, *The Bloch-Wigner-Ramakrishnan polylogarithm function*, *Math. Annalen* **286** (1990) 613.

[26] W. Duke and O. Imamoglu, *On a formula of Bloch*, in *The Deshouillers Birthday Volume*, *Funct. Approx. Comment. Math.* **37, Part 1** (2007) 109.

[27] A. Weil, *Elliptic Functions according to Eisenstein and Kronecker*, Ergebnisse der Mathematik und ihrer Grenzgebiete, vol. 88, Springer-Verlag (1976) [DOI].

[28] I. Aniceto, G. Basar and R. Schiappa, *A Primer on Resurgent Transseries and Their Asymptotics*, *Phys. Rept.* **809** (2019) 1 [arXiv:1802.10441] [INSPIRE].

JHEP09(2020)184

[29] S.S. Razamat, *On a modular property of $N = 2$ superconformal theories in four dimensions*, *JHEP* **10** (2012) 191 [arXiv:1208.5056] [INSPIRE].

[30] L. Di Pietro and Z. Komargodski, *Cardy formulae for SUSY theories in $d = 4$ and $d = 6$*, *JHEP* **12** (2014) 031 [arXiv:1407.6061] [INSPIRE].

[31] E. Shaghoulian, *Modular Invariance of Conformal Field Theory on $S^1 \times S^3$ and Circle Fibrations*, *Phys. Rev. Lett.* **119** (2017) 131601 [arXiv:1612.05257] [INSPIRE].

[32] C. Beem and L. Rastelli, *Vertex operator algebras, Higgs branches, and modular differential equations*, *JHEP* **08** (2018) 114 [arXiv:1707.07679] [INSPIRE].

[33] M. Dedushenko and M. Fluder, *Chiral Algebra, Localization, Modularity, Surface defects, And All That*, arXiv:1904.02704 [INSPIRE].

[34] F.A. Dolan and H. Osborn, *Applications of the Superconformal Index for Protected Operators and q-Hypergeometric Identities to $N = 1$ Dual Theories*, *Nucl. Phys. B* **818** (2009) 137 [arXiv:0801.4947] [INSPIRE].

[35] G. Felder and A. Varchenko, *The elliptic gamma function and* $\mathrm{SL}(3, Z) \times Z^3$, math/9907061.

[36] V.P. Spiridonov, *Elliptic beta integrals and solvable models of statistical mechanics*, *Contemp. Math.* **563** (2012) 181 [arXiv:1011.3798] [INSPIRE].

[37] V.P. Spiridonov and G.S. Vartanov, *Elliptic hypergeometric integrals and 't Hooft anomaly matching conditions*, *JHEP* **06** (2012) 016 [arXiv:1203.5677] [INSPIRE].

[38] V. Paşol and W. Zudilin, *A study of elliptic gamma function and allies*, arXiv:1801.00210 [INSPIRE].

[39] A. Levin, *Elliptic polylogarithms: An analytic theory*, *Compos. Math.* **106** (1997) 267.

[40] F.C.S. Brown and A. Levin, *Multiple Elliptic Polylogarithms*, arXiv:1110.6917.

[41] A. Sen, *Walls of Marginal Stability and Dyon Spectrum in $N = 4$ Supersymmetric String Theories*, *JHEP* **05** (2007) 039 [hep-th/0702141] [INSPIRE].

[42] A. Dabholkar, S. Murthy and D. Zagier, *Quantum Black Holes, Wall Crossing, and Mock Modular Forms*, arXiv:1208.4074 [INSPIRE].

[43] E. Witten, *Analytic Continuation Of Chern-Simons Theory*, *AMS/IP Stud. Adv. Math.* **50** (2011) 347 [arXiv:1001.2933] [INSPIRE].

[44] Z.-W. Chong, M. Cvetic, H. Lü and C.N. Pope, *General non-extremal rotating black holes in minimal five-dimensional gauged supergravity*, *Phys. Rev. Lett.* **95** (2005) 161301 [hep-th/0506029] [INSPIRE].

[45] J.B. Gutowski and H.S. Reall, *Supersymmetric AdS_5 black holes*, *JHEP* **02** (2004) 006 [hep-th/0401042] [INSPIRE].

[46] P. Basu, J. Bhattacharya, S. Bhattacharyya, R. Loganayagam, S. Minwalla and V. Umesh, *Small Hairy Black Holes in Global AdS Spacetime*, *JHEP* **10** (2010) 045 [arXiv:1003.3232] [INSPIRE].

[47] J. Markeviciute and J.E. Santos, *Hairy black holes in $AdS_5 \times S^5$*, *JHEP* **06** (2016) 096 [arXiv:1602.03893] [INSPIRE].

[48] J. Markeviciute, *Rotating Hairy Black Holes in $AdS_5 \times S^5$*, *JHEP* **03** (2019) 110 [arXiv:1809.04084] [INSPIRE].

JHEP09(2020)184

[49] R. Dijkgraaf, J.M. Maldacena, G.W. Moore and E.P. Verlinde, *A Black hole Farey tail*, hep-th/0005003 [INSPIRE].

[50] J.M. Maldacena and A. Strominger, *AdS_3 black holes and a stringy exclusion principle*, *JHEP* **12** (1998) 005 [hep-th/9804085] [INSPIRE].

[51] W. Nahm, A. Recknagel and M. Terhoeven, *Dilogarithm identities in conformal field theory*, *Mod. Phys. Lett. A* **8** (1993) 1835 [hep-th/9211034] [INSPIRE].

[52] H. Zagier and D. Gangl, *Classical and elliptic polylogarithms and special values of L-series*, in *The Arithmetic and Geometry of Algebraic Cycles, Proceedings, 1998 CRM Summer School*, Nato Science Series C, Vol. 548, Kluwer, Dordrecht-Boston-London, pp. 561–615.

[53] W. Nahm, *Conformal field theory and torsion elements of the Bloch group*, in *Les Houches School of Physics: Frontiers in Number Theory, Physics and Geometry*, pp. 67–132 (2007) [DOI] [hep-th/0404120] [INSPIRE].

[54] E. D'Hoker, M.B. Green, Ö. Gürdogan and P. Vanhove, *Modular Graph Functions*, *Commun. Num. Theor. Phys.* **11** (2017) 165 [arXiv:1512.06779] [INSPIRE].

[55] J. Broedel, O. Schlotterer and F. Zerbini, *From elliptic multiple zeta values to modular graph functions: open and closed strings at one loop*, *JHEP* **01** (2019) 155 [arXiv:1803.00527] [INSPIRE].

[56] F. Rodriguez Villegas, *Modular Mahler measures I*, in *Topics in Number Theory*, S.D. Ahlgren, G.E. Andrews, K. Ono eds., Kluwer, Dordrecht, pp. 17–48 (1999).

[57] G.W. Moore, *Arithmetic and attractors*, hep-th/9807087 [INSPIRE].

[58] E.W. Barnes, *On the theory of multiple gamma function*, *Trans. Cambridge Phil. Soc.* **19** (1904) 374.

[59] A. Narukawa, *The modular properties and the integral representations of the multiple elliptic gamma functions*, math/0306164.

[60] S.M. Hosseini, A. Nedelin and A. Zaffaroni, *The Cardy limit of the topologically twisted index and black strings in AdS_5*, *JHEP* **04** (2017) 014 [arXiv:1611.09374] [INSPIRE].

[61] J. Hong and J.T. Liu, *The topologically twisted index of $\mathcal{N} = 4$ super-Yang-Mills on $T^2 \times S^2$ and the elliptic genus*, *JHEP* **07** (2018) 018 [arXiv:1804.04592] [INSPIRE].

JHEP09(2020)184